

Review

Review on Integrated On-Board Charger-Traction Systems: V2G Topologies, Control Approaches, Standards and Power Density State-of-the-Art for Electric Vehicle

Shahid Jaman ^{1,2}, Sajib Chakraborty ^{1,2}, Dai-Duong Tran ^{1,2}, Thomas Geury ^{1,2}, Mohamed El Baghdadi ^{1,2} and Omar Hegazy ^{1,2,*}

- ¹ MOBI-EPOWER Research Group, ETEC Department, Vrije Universiteit Brussel (VUB), Pleinlaan 2, 1050 Brussels, Belgium; shahid.jaman@vub.be (S.J.); sajid.chakraborty@vub.be (S.C.); dai-duong.tran@vub.be (D.-D.T.); thomas.geury@vub.be (T.G.); mohamed.el.baghdadi@vub.be (M.E.B.)
² Flanders Make, Gaston Geenslaan 8, 3001 Heverlee, Belgium
* Correspondence: omar.hegazy@vub.be

Abstract: This article reviews the different topologies compatible with V2G feature and control approaches of integrated onboard charger (iOBC) systems for battery electric vehicles (BEVs). The integrated topologies are presented, analyzed, and compared in terms of component count, switching frequency, total harmonic distortion (THD), charging and traction efficiencies, controllability, reliability and multifunctionality. This paper also analyzes different control approaches for charging and traction modes. Moreover, the performance indices such as setting time, rise time, overshoot, etc., are summarized for charging and traction operations. Additionally, the feasibility of a Level 3 charging (AC fast charging with 400 Vac) of up to 44 kW iOBC is discussed in terms of converter efficiencies with different switching frequencies and switch technologies such as SiC and GaN. Finally, this paper explores the power density trends of different commercial integrated charging systems. The power density trend analysis could certainly help researchers and solution engineers in the automotive industry to select the suitable converter topology to achieve the projected power density.

Keywords: bidirectional EV charger; integrated on-board battery chargers (iOBCs); charging control; V2G charger



Citation: Jaman, S.; Chakraborty, S.; Tran, D.-D.; Geury, T.; El Baghdadi, M.; Hegazy, O. Review on Integrated On-Board Charger-Traction Systems: V2G Topologies, Control Approaches, Standards and Power Density State-of-the-Art for Electric Vehicle. *Energies* **2022**, *15*, 5376. <https://doi.org/10.3390/en15155376>

Academic Editor: Hugo Morais

Received: 24 June 2022

Accepted: 22 July 2022

Published: 25 July 2022

Publisher's Note: MDPI stays neutral with regard to jurisdictional claims in published maps and institutional affiliations.



Copyright: © 2022 by the authors. Licensee MDPI, Basel, Switzerland. This article is an open access article distributed under the terms and conditions of the Creative Commons Attribution (CC BY) license (<https://creativecommons.org/licenses/by/4.0/>).

1. Introduction

Electric vehicles (EVs) are the most competitive and promising transportation solution compared to internal combustion engine (ICE) vehicles due to their impact on carbon neutrality and resource efficiency [1]. To achieve ambitious EU Green deal targets, automotive Original Equipment Manufacturers (OEMs) aim to sell 100% of zero-emission cars from 2030 onwards [2,3]. According to the Global EV outlook 2021, the global EV market for all types of car sales was significantly affected by the economic repercussions of the COVID-19 pandemic. One-third of new car registrations dropped in the first part of 2020 when compared to the preceding year [4]. Though overall new car registration was falling, global EV car sales increased by up to 70% as 3 million new EV cars were registered in 2020, which was a record 4.6% annual growth. For the first time, Europe led with 1.4 million new registrations. China followed with 1.2 million registrations, while the number of new registration in the United States was 295,000 [4], as shown in Figure 1. Two aspects are essential to sustain exponential EV growth and sales demand. First, developing chargers and the availability of fast charging options need to be confirmed. Second, the bidirectionality, performance, and lifetime of the existing charger topologies must improve so that EV charging becomes more affordable and reliable [5].

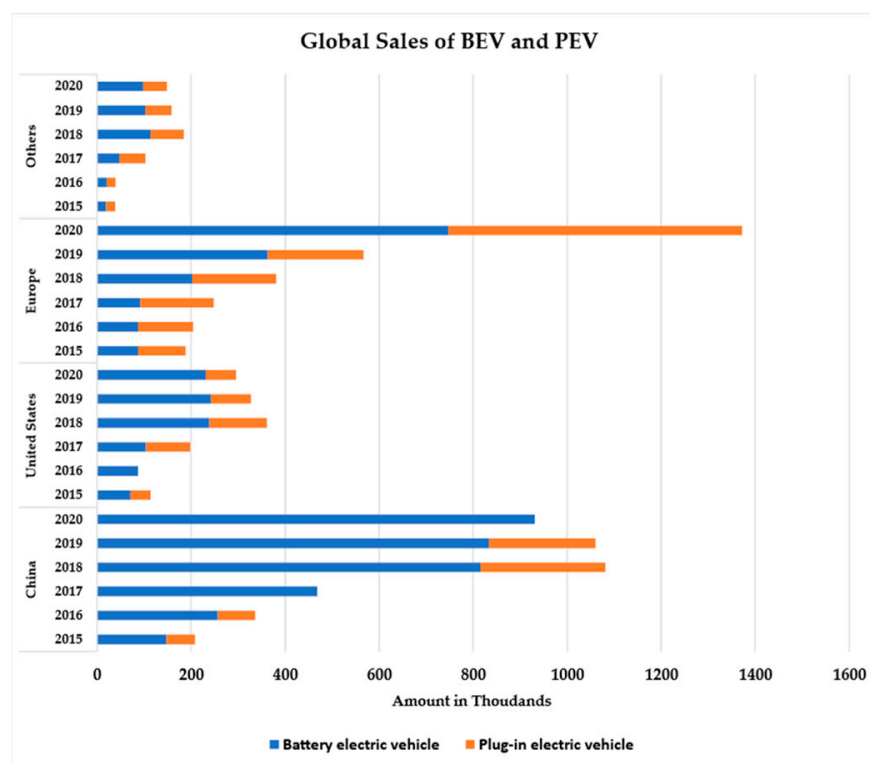


Figure 1. Electric vehicle sales (in thousands) in 2015–2020 (blue is used for BEV and orange for PEV) [4].

Two types of chargers are widely used for EV charging, i.e., on-board chargers (OBC) and off-board chargers. OEMs are still facing problems in the OBC as they are still expensive, bulky, and offer only unidirectional power flow (e.g., grid-to-vehicle (G2V)) [6,7]. To obtain higher power density, OEMs have headed towards integrated bidirectional OBC that could offer a more efficient and power-dense solution. Thus, due to the bidirectional features of OBCs, vehicle-to-grid (V2G) functionality can be achieved, which can transfer electrical energy back to the grid during peak demand [8].

Moreover, bidirectional features allow more functionalities in OBCs, such as vehicle-to-home (V2H), vehicle-to-device (V2D), or vehicle-to-vehicle (V2V), which leads to an increase in the power transfer capability [9]. However, power transfer capability is typically limited due to several constraints/tradeoffs such as cost, volume, and weight of the vehicle [10]. The iOBCs can help to overcome these limitations, as iOBCs build a closer integration of the motor and power electronics components (i.e., electric motor and traction inverter) for charging instead of using separate power electronics stages (e.g., AC/DC and DC/DC) and bulky inductors, as shown in Figure 2.

With the charging system shown in Figure 2, the iOBCs use the motor windings as a filter inductance to improve the grid current quality. In addition, in iOBC topologies, the propulsion inverter serves as an active front end (AFE) bidirectional AC/DC converter during charging. Due to the usage of a high-power inverter as a AFE AC/DC converter, the iOBC's charging power level is increased beyond state of the art (i.e., 43 kW). The status of charging and motor power levels of recent car models are listed in Table 1. However, OEMs face technical challenges such as winding reconfiguration, torque production during charging, high charging current THD and torque ripples to provide such a high power charging facility with iOBC technologies [11,12]. To overcome these technical problems, OEMs are using advanced motor, power converter technologies and robust charging and traction control strategies. Moreover, they also use safety and charging ports standards as shown in Table 2 for protection against abnormal system touch potential and leakage current. On the other hand, researchers are solving these technical problems using power

stage integration in charging systems to achieve a high charging power level. They are using multiple stage power conversion to transfer the charging power to the EV battery. For example, higher-level integration has been adopted by Nissan Leaf which reflects a compact design of the EV powertrain components (i.e., battery, e-motor, power electronics and thermal management modules) [12]. Moreover, Tesla and Volkswagen (VW) are also integrating the power stages and motor drive to achieve a better power density. Car manufacturers and researchers are improving the iOBC power densities with greater efficiency, of range coverage and a flexible charging strategy to attract more customers [13]. Indeed, the iOBC solution has positively impacted volume, weight, and efficiency, reduced car production cost, and increased the overall driving range [14,15]. A significant study has been conducted on iOBC topologies and control strategies that are being adopted in many research works [16–19].

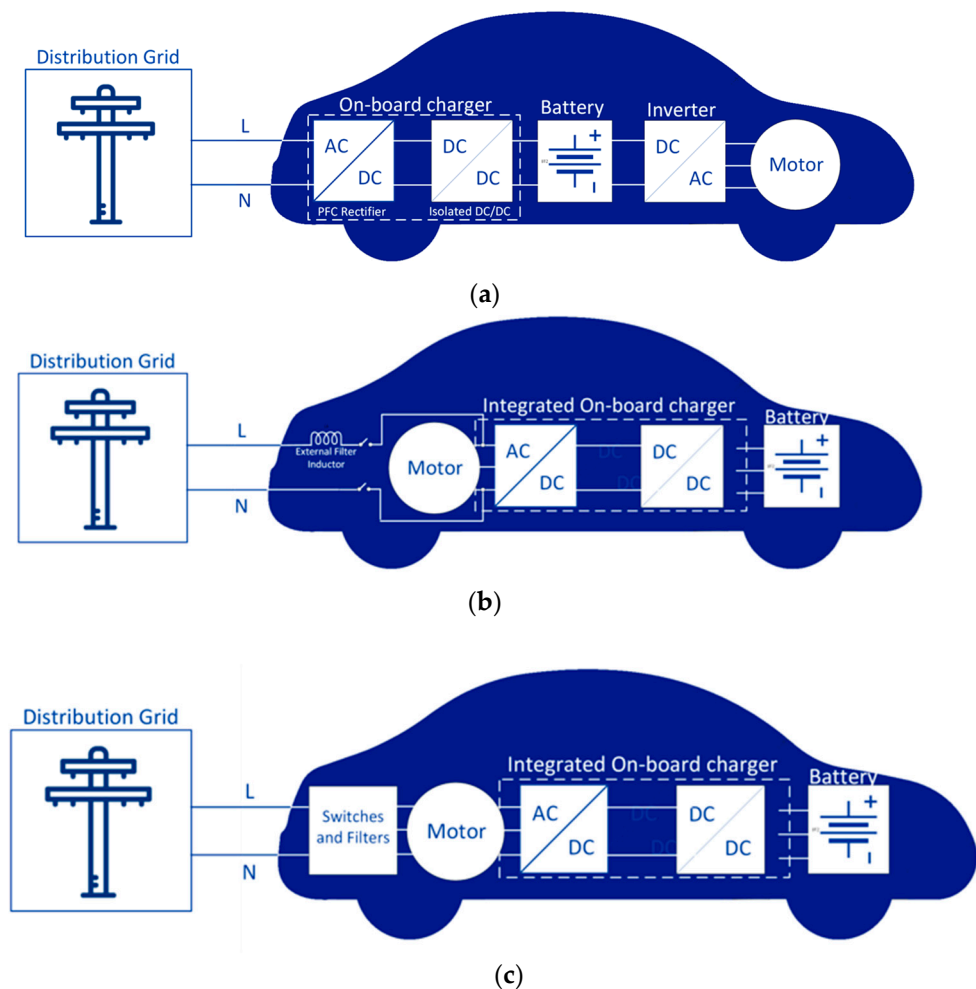


Figure 2. On-board power electronic interfaces for EV Charging. (a) Conventional on-board charging system. (b) Integrated on-board charger system with external filter inductor for grid. (c) Integrated on-board charger system with motor coil as filter inductor for grid.

All the available literature reviews on iOBCs focus on the power stages, (i.e., topologies, control strategies, and challenges). However, the following research gaps are identified in the existing studies: (a) a comprehensive analysis of the recently developed bidirectional iOBC topologies; (b) a detailed investigation of the control strategy used in different modes of iOBCs; (c) a discussion of EV charging standards and power density trends. In this context, this paper presents a review of the iOBCs proposed in the literatures and patents, as well as a comparison between them, both in terms of implementation requirements (e.g., the need for external inductors or contactors) and functionalities (e.g., galvanic isolation,

bidirectional operation). Moreover, a novel and detailed qualitative and quantitative analysis is performed for each, including losses and efficiency. In support, this work presents the following contributions:

- Detailed analysis of the recently developed bidirectional iOBC topologies including advantages, disadvantages, available features, and efficiencies with different switch technologies.
- Comparative investigation of charging and driving mode control strategies used in iOBCs including overshoot and dynamic response.
- Summary of the requirements and estimated power density trends of commercial integrated charging solutions.

Table 1. Electric powertrain specification of commercially available EVs.

Region	Year	EV Model	Ref.	Motor Power (kW)	Battery Capacity (kWh)	Charging Time	Max. OBC Rating (kW)
Europe	2021	Hyundai IONIQ 5	[20]	160	73	6 h 9 min	11
	2021	BMW X3	[21]	125	43	3 h 15 min	11
	2021	Nissan Leaf	[22]	110	40	3 h 22 min	11
	2021	VW ID4 Pro S	[23]	150	82	7 h 30 min	11
	2021	Audi e-Tron	[24,25]	230	71.2	7 h 07 min	11
	2020	Renault Zoe R135	[26]	100	54.66	2 h 22 min	43
	2021	Mercedes Benz EQA	[27]	140	66.5	5 h 45 min	11
US	2021	Tesla Model Y	[28,29]	201	75	7 h 30 min	11/22
	2021	Chevy Bolt	[30]	150	66	10 h	6.6
	2021	Porsche Taycan Turbo S	[31,32]	190	93.4	10 h 30 min	11
China/ Japan	2017	BAIC EC180	[33]	30	22	2 h 14 min	11
	2020	Chery eQ	[34]	30	32	3 h 14 min	11
	2019	JACK iEV7 S/E	[35]	50	24	2 h 26 min	11
	2017	JMC E200	[36]	30	17.3	1 h 45 min	11

Table 2. Charging power level standards and configurations adapted from [37].

Charging Level	Voltage Level	Max Power (kW)	Charging Time	China	Europe	Japan	North America
Level 1	120 VAC	3.7	10–15 h	Private Outlet (Not Specific for EVSE)			SAE J1772 T1
Level 2	220 VAC	3.7–22	3.5–7 h	GB/T 20234 AC	IEC 62196 T2	SAE J1772 T1	SAE J1772 T1
Level 3	480 VAC (US)/ 400 VAC (EU)	22–43.5	10–30 min	GB/T 20234 AC	IEC 62196 T2		SAE J3068
	200–600 DC	<200 <150	10–30 min	GB/T 20234 DC	CCS Combo 2	CHAdeMO	CCS Combo 1
XFC	>800 VDC	>400	H ₂ Gas refueling		CCS/CHAdeMO		

This review paper is organized as follows: Section 1 describes the present scenarios for EV sales and the electric drivetrain and its components and discusses the global charging infrastructure, including available charging ports. Section 2 explains drivetrain components, control, and cooling integration strategies. Section 3 describes the literature review for iOBC with different power electronic modules. Section 4 explains the control strategies and performance comparison for charging and driving modes of iOBCs. Section 5 illustrates the detailed comparison analysis comparing iOBC topologies. Section 6 describes the electric vehicle charging standards which need to be maintained during iOBC installations. Section 7 discusses the status of power densities of integrated drivetrain and chargers used by the car manufacturers and OEMs. Section 8 explains the economic and environmental

aspects of mass incorporation of the integrated onboard charger in the market. Finally, Section 9 concludes the review work with outlooks and discussion.

2. On-Board Charger Integration Methods

In most traditional EV powertrain systems, the battery charger and motor propulsion unit are separate, so two independent circuits are operating during two different operations. Thus, EVs need more space on-board to accommodate these units which leads to higher weight and modular losses. Integrated on-board chargers (iOBCs) can provide flexibility for layout space, cost, and weight, so that EVs can obtain better efficiency and high-power densities. There are three common approaches to implement on-board charger integration and achieve high power density by combining the powertrain, control circuit and mechanics.

OBC integration with a high voltage DC/DC converter is one of the most common approaches to integration, as shown in Figure 3b,d. In this approach, both modules share the same base plate as well as the cooling and control board [38–44]. Some analyses have shown that the cost of a single integrated OBC and DC/DC unit is 19% lower than the cost of having two separate units [45]. The OBC and high-voltage DC/DC converter are connected to a high-voltage battery, so the rated voltage of the full bridge is the same for the onboard charger and the high-voltage DC/DC. This enables power-switch sharing with the full bridge for both the onboard charger and the high-voltage DC/DC. The second integration approach is OBC unit integration with traction inverter, as depicted in Figure 3c. Generally, the inverter unit is a separate module with dedicated cooling and control board. The integrated unit comprises the same power and cooling unit. Some motor drive integrated OBC systems use the same control unit [46–50]. Additionally, this kind of integration leads to the cost reduction and power-density improvement of this design [51,52]. However, a good operating mode transition strategy is needed. power stage integration with mechanical housing and control is the most compact solution of all, as shown in Figure 3e. This is also known as a highly integrated solution for PE modules. This approach can give the least volume for the integrated solution. A high level integrated system (i.e., OBC, traction inverter and DC/DC) are available in the latest literature [53]. The motoring mode operation is not observed, but the V2G operation is experimented with to send the power back to the grid. However, many challenges can arise during implementation of such an integrated solution, such as control and cooling complexity, EMI and THD issues, zero torque problem during charging, battery isolation from the grid, etc.

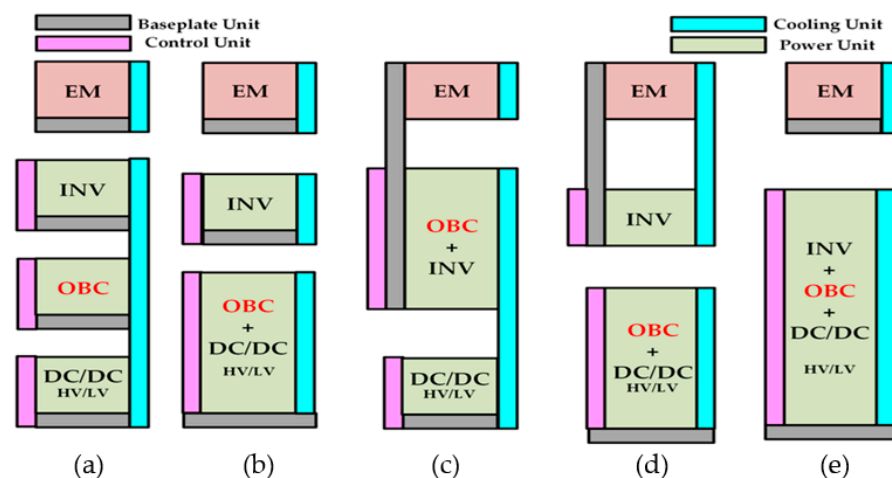


Figure 3. Power/PCB Unit integration approaches. (a) Separated power units, (b) OBC and DC/DC power unit integration with separate motor drive unit, (c) Integrated power unit for OBC and motor drive, (d) Power unit integration for OBC and DC/DC unit with separately controlled motor drive, (e) Integration of motor drive, OBC and DC/DC control unit.

The prototype implementation of such integrated PE systems are listed in Table 3 below with advantage and disadvantages.

Table 3. Integrated OBC state-of-the-art prototypes.

Ref.	Integration Type	OBC Power	Inverter/DCDC Power	Shared Components	Switch Tech.	Advantages	Disadvantages
[54]	OBC-DCDC	22 kW	3.7 kW	1. Mechanical Housing 2. Power PCB 3. Control PCB 4. Cooling Plate	SiC	1. Charging flexibility 2. Galvanic isolated power transfer 3. Reduced volume	1. Not compatible for 3-ph grid supply 2. DC/DC power is low
[55]	OBC-DCDC	11 kW	3 kW	1. Mechanical Housing. 2. Power PCB 3. Control PCB 4. Cooling Plate	Si	1. Charging flexibility. 2. Less weight which is around 10 kg 3. Reduced volume which is around 0.0134 L	1. Unable to fit 800 V battery charging 2. Complex control system.
[56]	OBC-INV	3.3 kW	-	1. Mechanical Housing. 2. Power PCB 3. Control PCB 4. Cooling Plate	SiC	1. Range increase around 10% 2. Low cost, weight, and volume 3. Motor winding used as grid filter	1. Low Power rating. 2. Low switching frequency
[57]	OBC-INV	43 kW	120 kW	1. Mechanical Housing. 2. Power PCB 3. Control PCB 4. Cooling Plate	SiC	1. Greater charging flexibility 2. High power AC and DC charging 3. Motor winding used as grid filter. 4. Integrated grid interface	1. Current THD is high. 2. High torque ripple. 3. Additional relay required for motor winding configuration

3. Integrated On-Board Charger (iOBC) Topologies

The iOBCs can be classified into isolated and non-isolated, as illustrates in Figure 4. Most non-isolated iOBCs use AC line as an input, using the motor winding. Each leg of the traction inverter is connected to each phase of motor winding. Thus, the inverter can be used as an active front-end (AFE) rectifier during charging. The non-isolated iOBC can also be built using a three phase and multiphase machine. Single three phase motor based iOBCs have been investigated in [58–60]. In these works, two operations (charging and traction) have been tested.

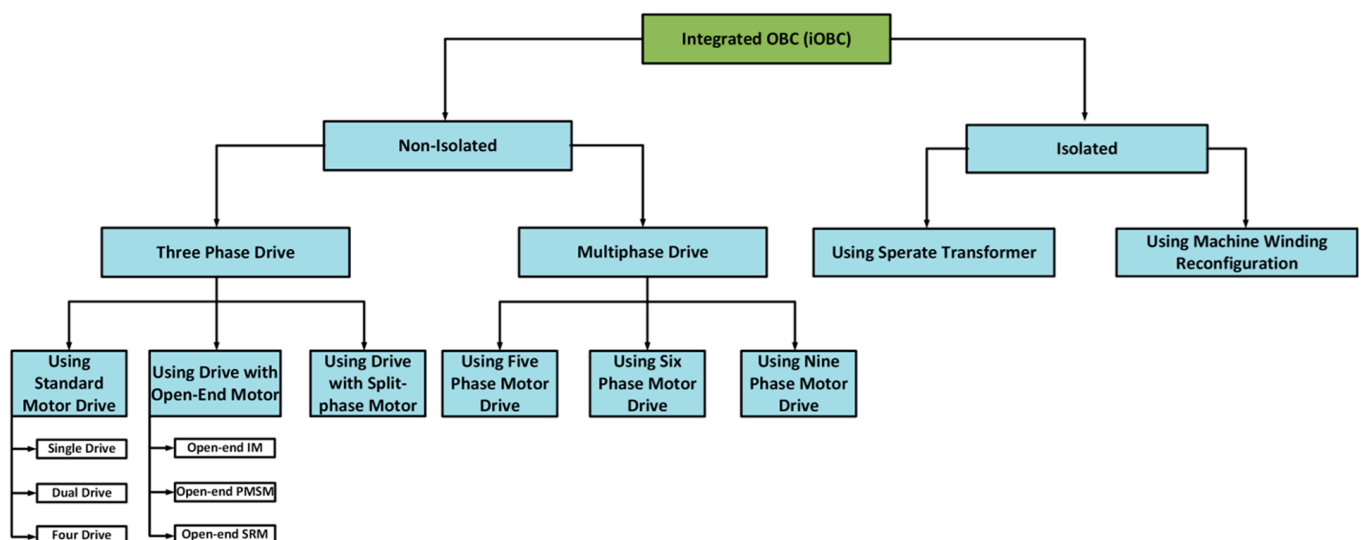


Figure 4. OBC integrated PE converter system topology classification.

These topologies use a contactor switch as shown in Figure 5 to connect the grid supply to the neutral point of the machine winding [61]. The stator winding can be utilized as a grid side filter. The motor uses symbols R and L_f as stator resistance and inductance, respectively. The main drawback of this topology is the current stress on the one leg, which is three

times higher than on the other converter legs. Another single-phase charging solution with two IMs and two sets of dedicated converters is described in [62] (see Figure 6). The power from the battery is transferred to both motors, hence the driving torque is shared by them. An improved interleaving switching based integrated charger based on a two-motor drive was introduced in [63]. Two slow recovery diodes, D_1 and D_2 , are added to alleviate the CM noise. As each diode provides a low-frequency path for the input current, the system ground is connected to the input terminal. Additional boost inductors, L_1 and L_2 , are utilized for the purpose of compensating for the small CM inductance. This technique effectively improves the efficiency and current waveforms concurrently. Four motor iOBCs are also suitable for single phase supply, described in [64,65]. For the mode to take place it is necessary to disconnect the positive terminal of the battery from the dc-bus and to connect it to two isolated neutral points of two machines, as shown in Figure 7.

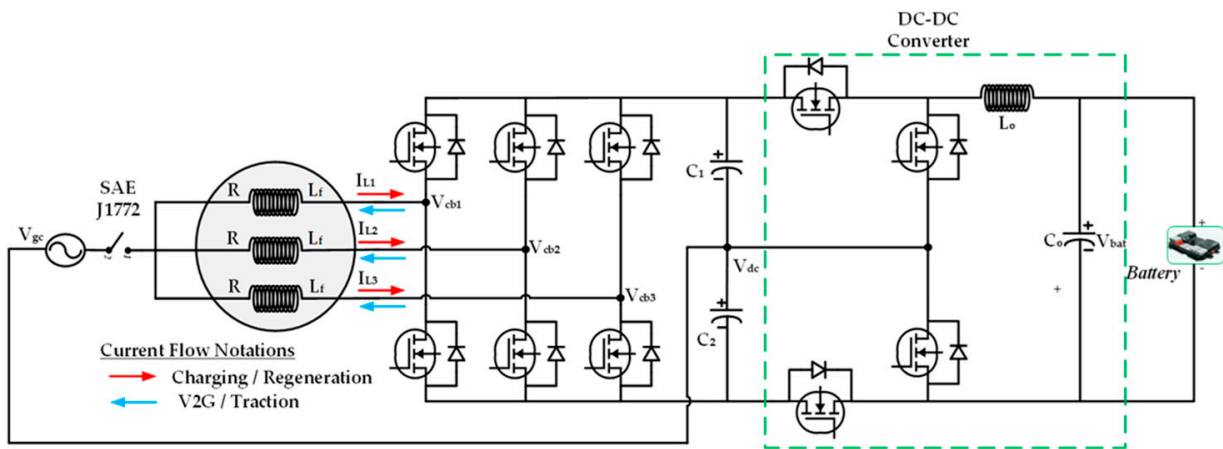


Figure 5. Single motor drive integrated on-board charger proposed by Gupta et al. [61] in 2020 (iOBC1).

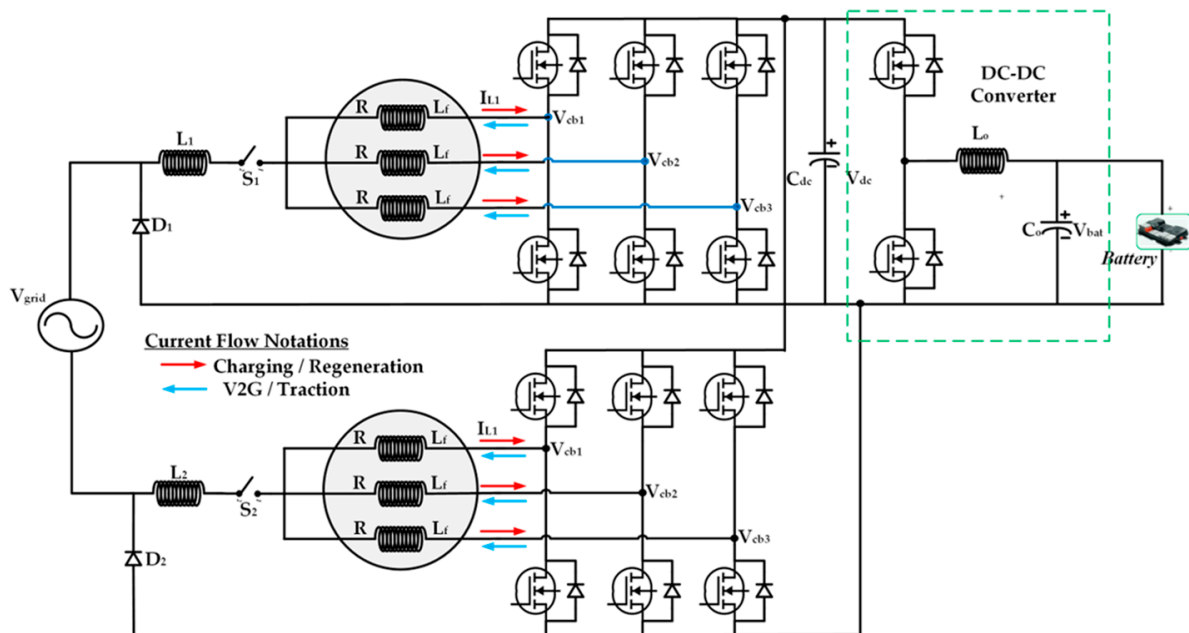


Figure 6. Dual motor drive integrated on-board charger proposed by Woo et al. [62] in 2015 (iOBC2).

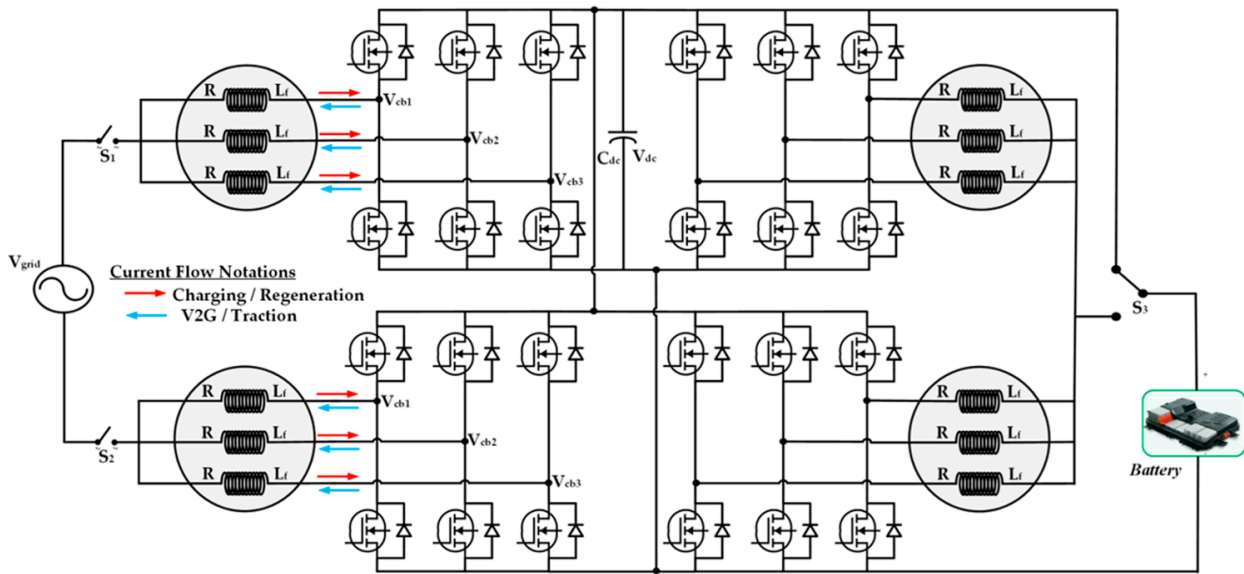


Figure 7. Four motor drive integrated on-board charger proposed by Subotic et al. [64] in 2014 (iOBC3).

A single-phase traction inverter integrated OBC is proposed in [66] (see Figure 8). For the charging mode from a single-phase grid, the traction inverter is configured as full bridge rectifier and inverter boost converter, using switches' S_1 to S_5 configuration to connect the battery. This topology has a very simple structure and control, V2G features and small size.

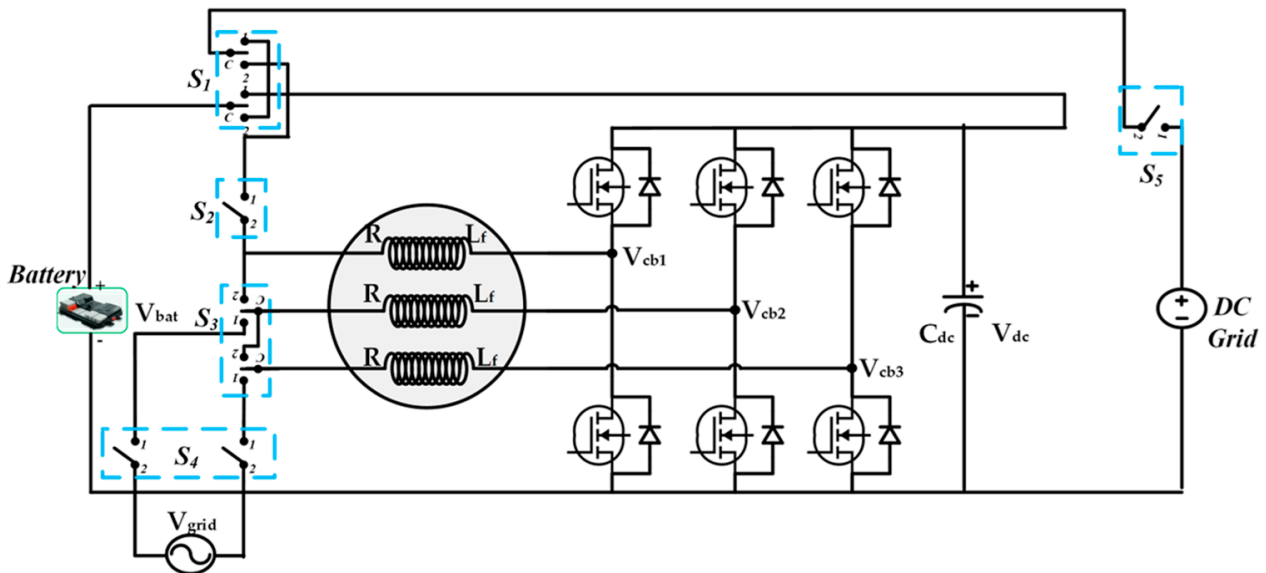


Figure 8. Induction motor drive integrated on-board charger with motor winding reconfiguration proposed by Khan et al. [66] in 2012 (iOBC4).

A PMSM drive integrated charging system has been introduced in [67] for electric motorcycle application. A rectifier and line filter used as an extra component in this system is depicted in Figure 9. A four-phase synchronous reluctance motor (SRM) winding is utilized in the iOBC system described in [68], as shown in Figure 10. This topology used one bridge of the inverter as a buck-boost converter and the other two bridges as a rectifier. The V2G and G2V functionalities of SRM drive iOBC have been explained in [69]. At first, two converter phases are utilized as a rectifier, with machine windings being employed as input filters. Then, when the grid voltage is rectified, the third phase acts as a dc-dc buck-boost

converter to adjust the voltage to a value required by the battery. The fourth phase is not used during the charging process. To reduce switching losses, switch S_4 is set permanently. There is no separate DC-DC converter for charging the battery in this topology, which gives simple reconstruction flexibility. Thus, the cost and size of the charger system decrease.

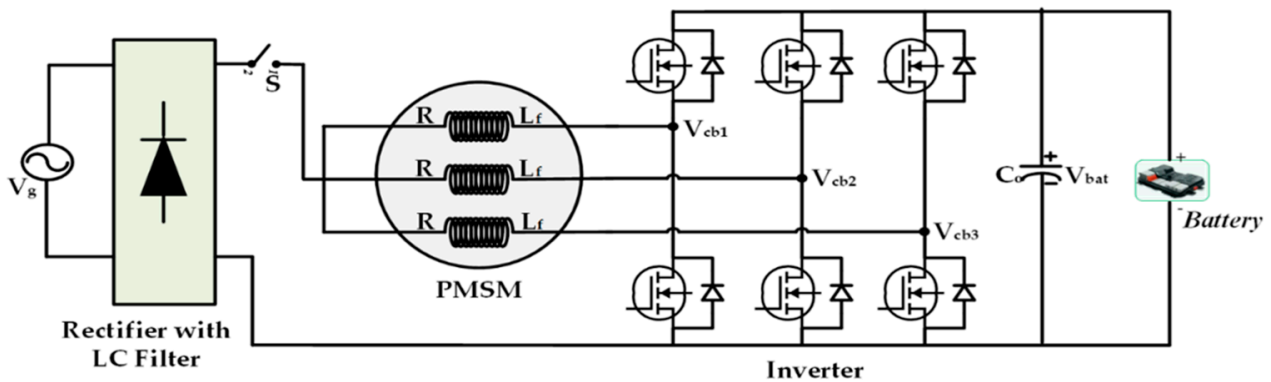


Figure 9. PMSM drive integrated on-board charger with neutral point access proposed by Tuan et al. [67] in 2021 (iOBC5).

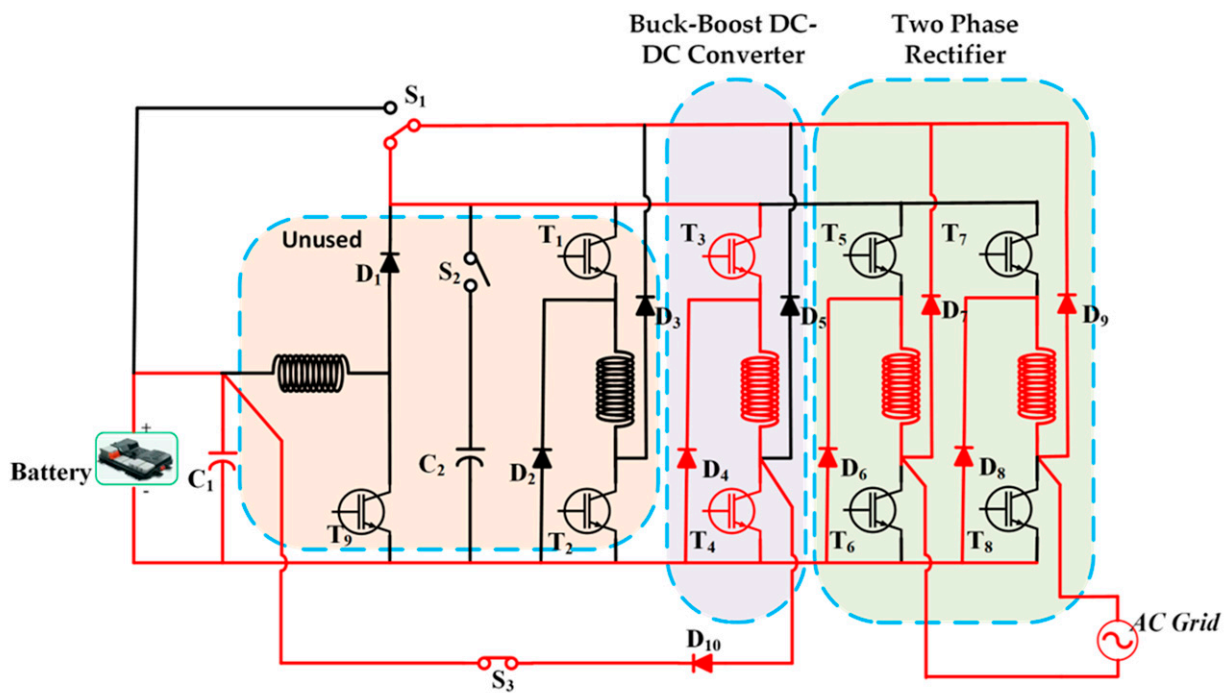


Figure 10. SRM drive integrated on-board charger proposed by Khayam Huseini et al. [68] in 2015. (iOBC6). The charging mode configuration is highlighted in red.

A cost effective 3-ph on-board charging system with interfaced converter is depicted in [70] and shown in Figure 11. The specific role of the interfaced converter in this topology is to configure the system during operating mode. Due to its simplicity, it allows high-power charging with comparatively less size and weight. An additional three-phase interface converter is used to avoid hardware reconfiguration. A fast three-phase charging system based on a split phase machine has been described in [71–75] and is shown in Figure 12. The mid-point of three phase winding is connected to the grid through an EMI filter and a H-bridge front-end converter with a battery connected to the machine. The main disadvantages of this topology are stator leakage inductance due to employed distributed

winding, and complexity in control. An integrated on-board charger with open-end stator winding (OEW) configurations of three-phase IM is described in [76,77].

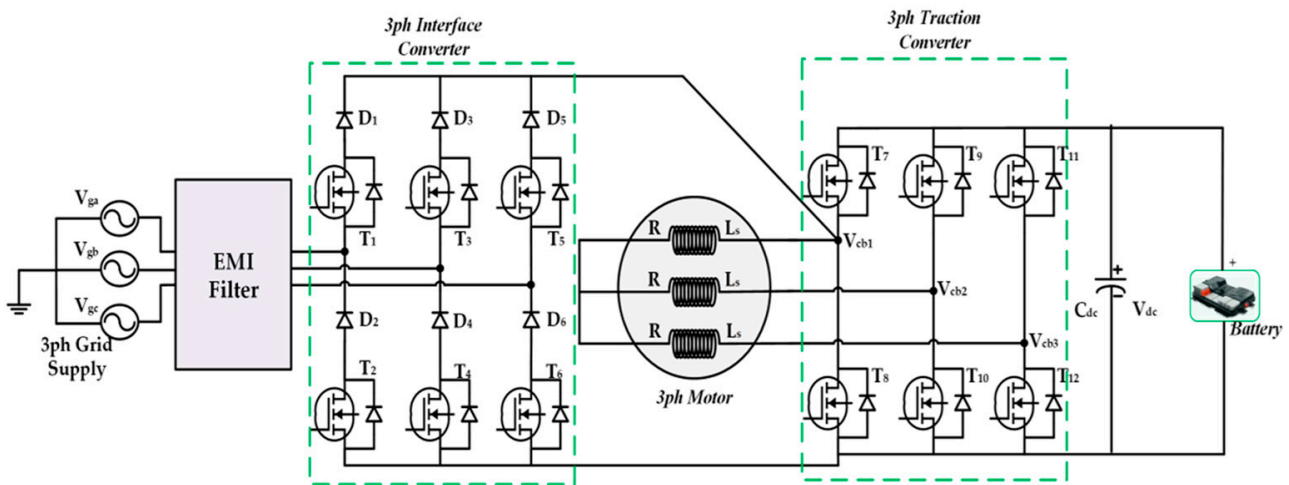


Figure 11. Three Phase integrated on-board charger with interface converter proposed by Shi et al. [70] in 2018. (iOBC7).

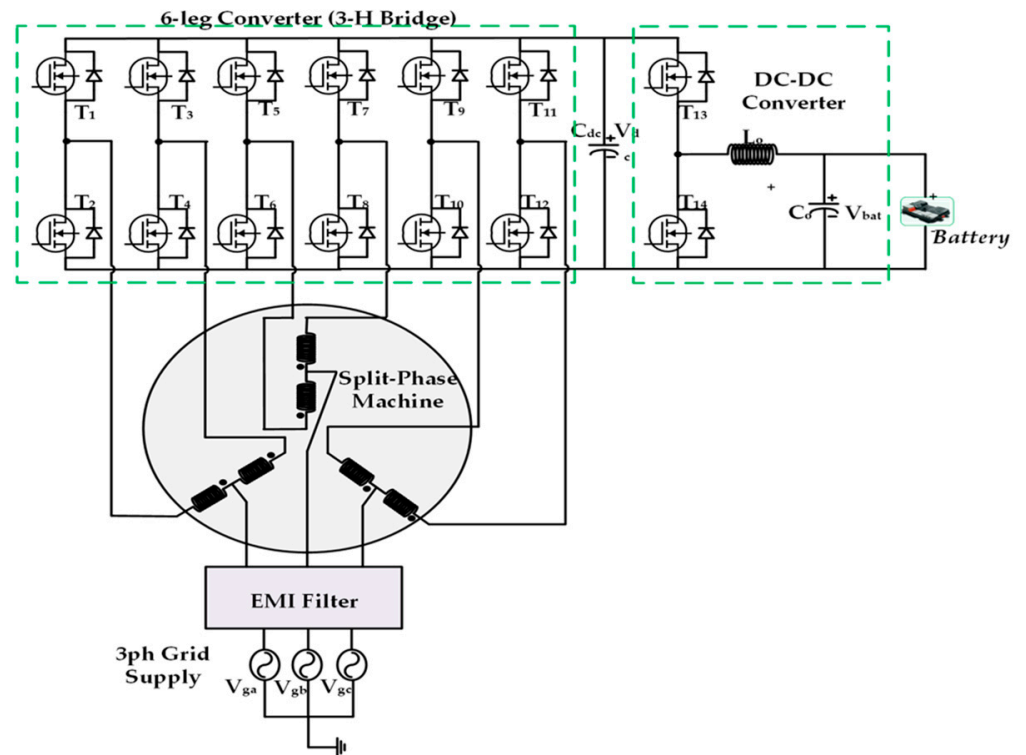


Figure 12. Three Phase Split-Phase Motor integrated on-board charger proposed by Hagbin et al [74] in 2014 (iOBC8).

The stator winding reconfiguration of these topologies can be carried out by using a switch as shown in Figure 13. Recently, Hyundai published a patent for a multi-charging system which is used in the Hyundai IONIQ 5 model, based on a OEW machine [78]. Another similar approach with asymmetrical hybrid multilevel converter as described in [79]. The OEW machine was also utilized to implement a dual drive integrated charger in [80,81].

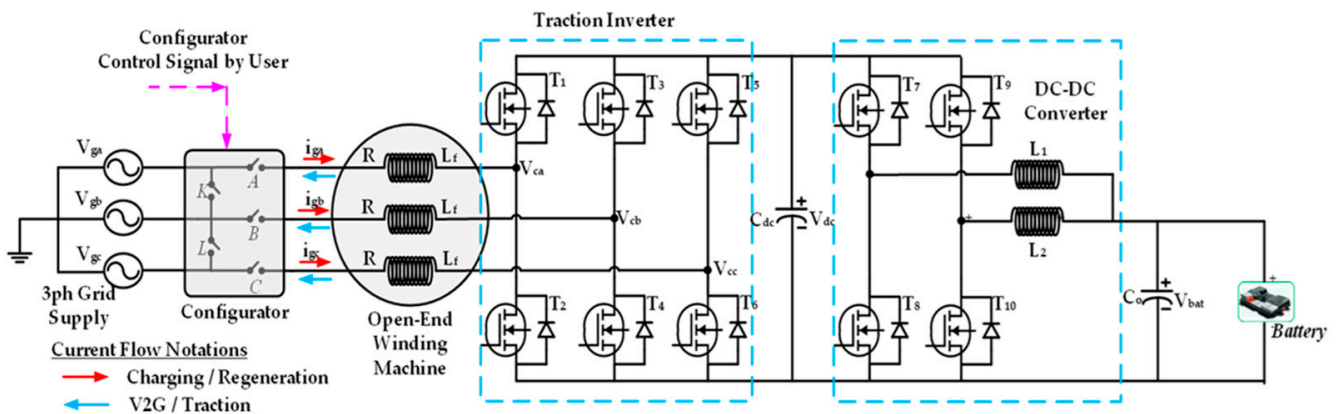


Figure 13. Integrated On-Board Charger based on Open-End Winding Machine proposed by Brull et al. [76] in 2016 (iOBC9).

Recently, segmented winding based three phase induction machines have caught researcher’s attention. This type of multi-winding machine is derived from the traditional three-phase machine, using the same number of stator slots and rotor poles. Various segmented three-phase machines have been reported in the literature, including the three-phase six-winding machine as shown in Figure 14 reported in [40,82], and the three-phase nine-winding machine depicted in Figure 15 and described in [83,84]. Multiphase machines have more than three phases; typically five, six and nine. They are categorized in two types as symmetrical and asymmetrical machines based on the spatial angle of two consecutive machine phases. They can have one or multiple isolated neutral points. The nine phase machines have higher torque and lower copper loss than six phase machines. The nine phase machine based iOBC topologies are investigated in [85,86].

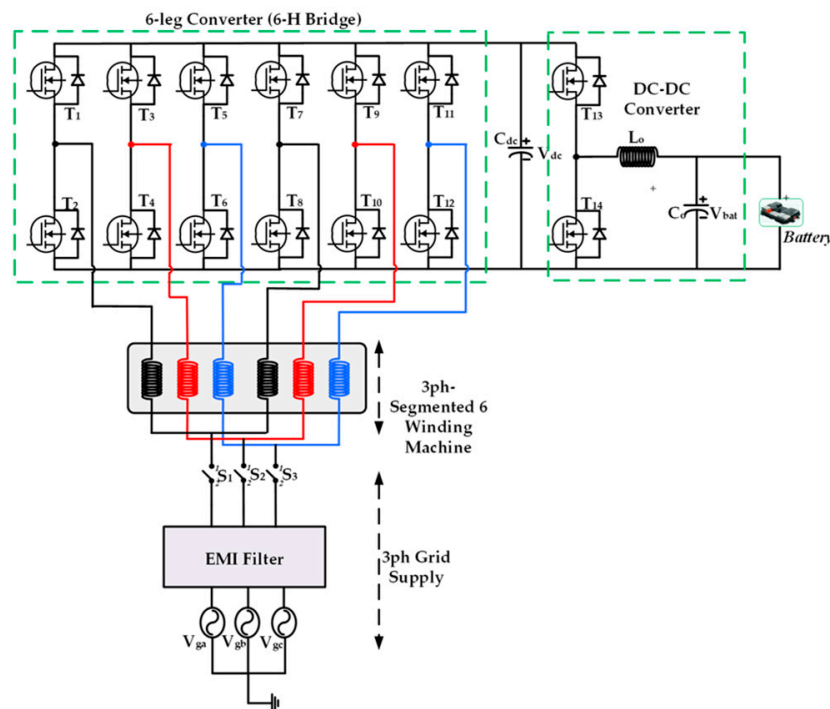


Figure 14. Integrated On-Board Charger based on 3-Phase 6-Segmented Winding Machine proposed by Han et al. [82] in 2018. (iOBC10).

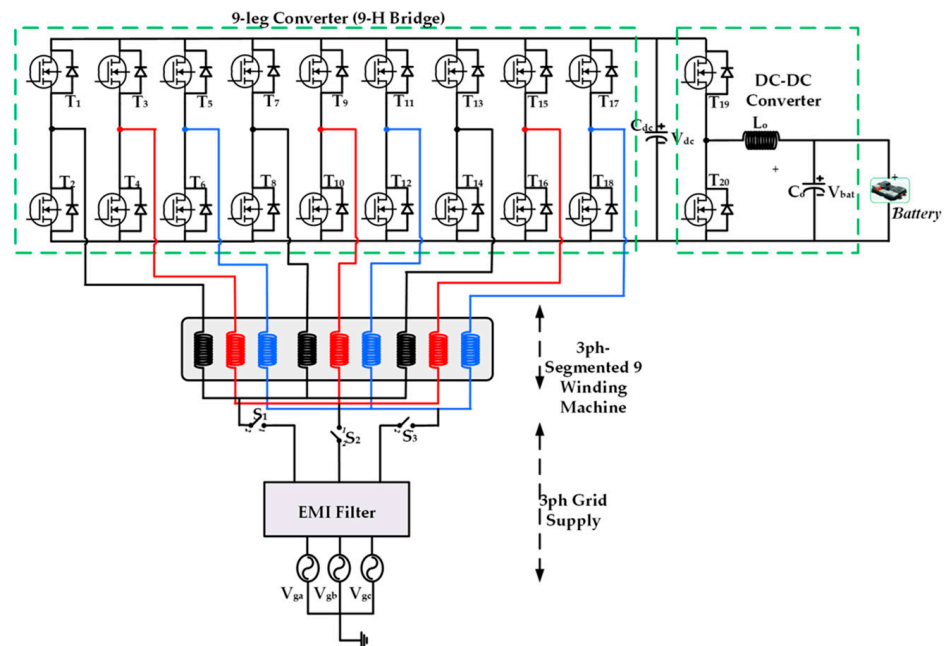


Figure 15. Integrated On-Board Charger based on 3-Phase 9-Segmented Winding Machine proposed by Raherimihaja et al. [83] in 2018 (iOBC11).

Since these topologies have a higher phase inverter as shown in Figure 16, a significant drawback of these converters is the relatively higher number of semiconductor switches and the complexity of the corresponding driving circuit. An impressive solution was introduced in [87] to reduce the number of switches.

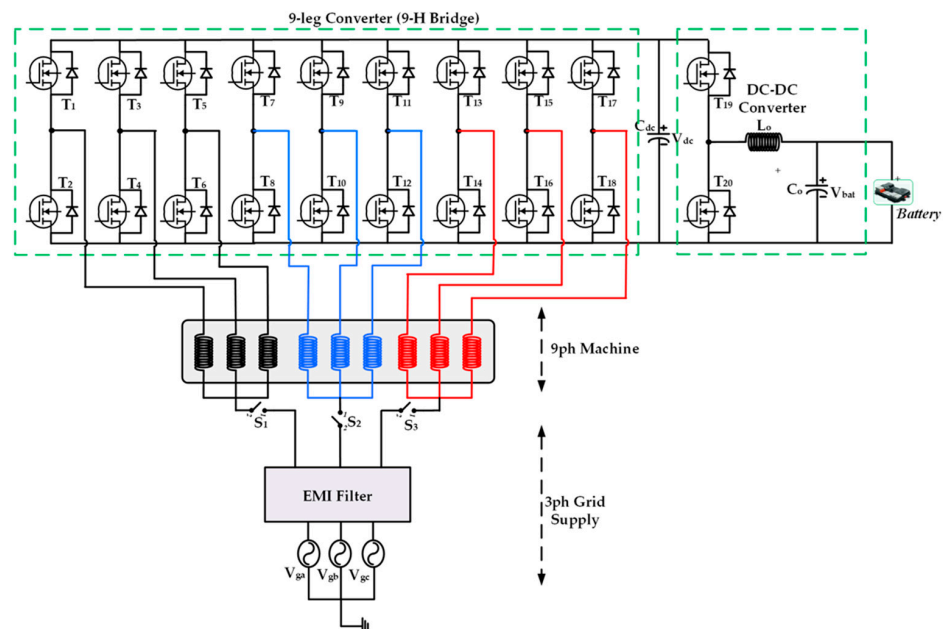


Figure 16. Integrated On-Board Charger based on Nine Phase Winding Machine proposed by Abdel-Khalik et al. [84] in 2017 (iOBC12).

The nine-switch converter was utilized with six phase machines as shown in Figure 17, where the stator coils act as filter during charging. The advantages of this topology are zero torque production during charging, the power factor is unity at the grid side and no phase transposition is needed. Additionally, only three additional switches are

needed for changing the mode. The most challenging drawback is the utilization of low dc-link capacitance.

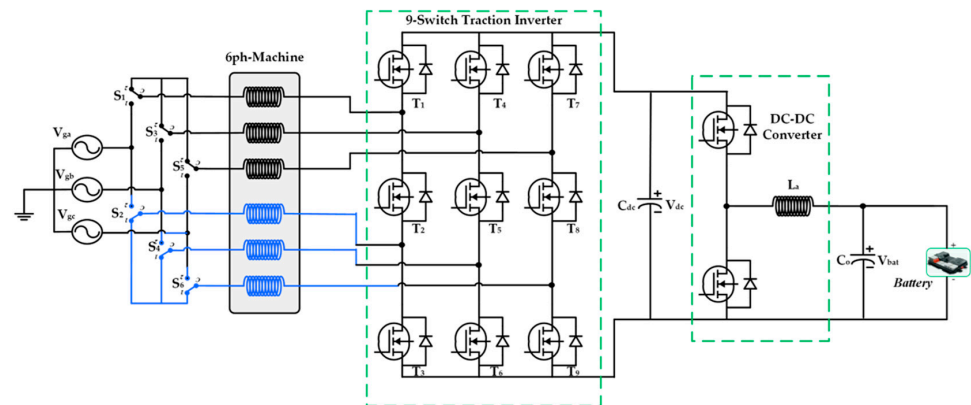


Figure 17. Integrated On-Board Charger based on Nine Phase Six Phase Winding Machine proposed by Diab et al. [87] in 2016. (iOBC13).

A five-phase machine approach (non-isolated method) as shown in Figure 18 is described in [88–90]. An efficiency analysis of the various integrated charger topologies shows that a nine-phase charger corresponds to the highest efficiency (reaching 86% during the charging mode). During charging, the efficiency varies from 79% to 86% based on the applied topology, while the efficiencies are slightly higher, between 81% and 89%, during the V2G mode. On the other hand, the isolated iOBCs can be implemented in two methods. One method can provide galvanic isolation by an additional transformer placed on the low-frequency AC side, as in [91]. Otherwise, the electrical isolation can be performed by reconfiguring the connections of the electrical machine to make it act as a transformer, which is proposed in [92,93], with six-phase and a nine-phase machines, respectively. In [94], a six-phase machine is used as transformer as shown in Figure 19 and provides galvanic isolation in both three- and single-phase input operation, with the peculiarity of achieving torque-free charging in single-phase configuration.

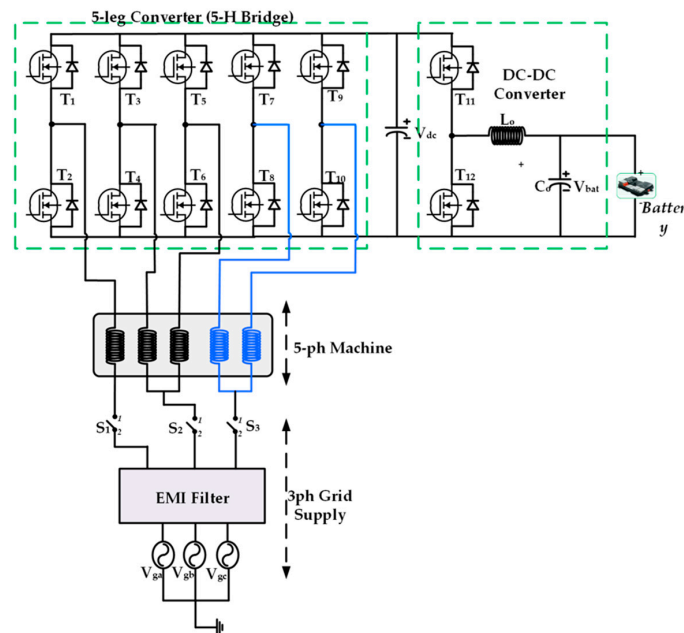


Figure 18. Integrated On-Board Charger based on Five Phase Winding Machine proposed by Sabotic et al. [88] in 2016 (iOBC14).

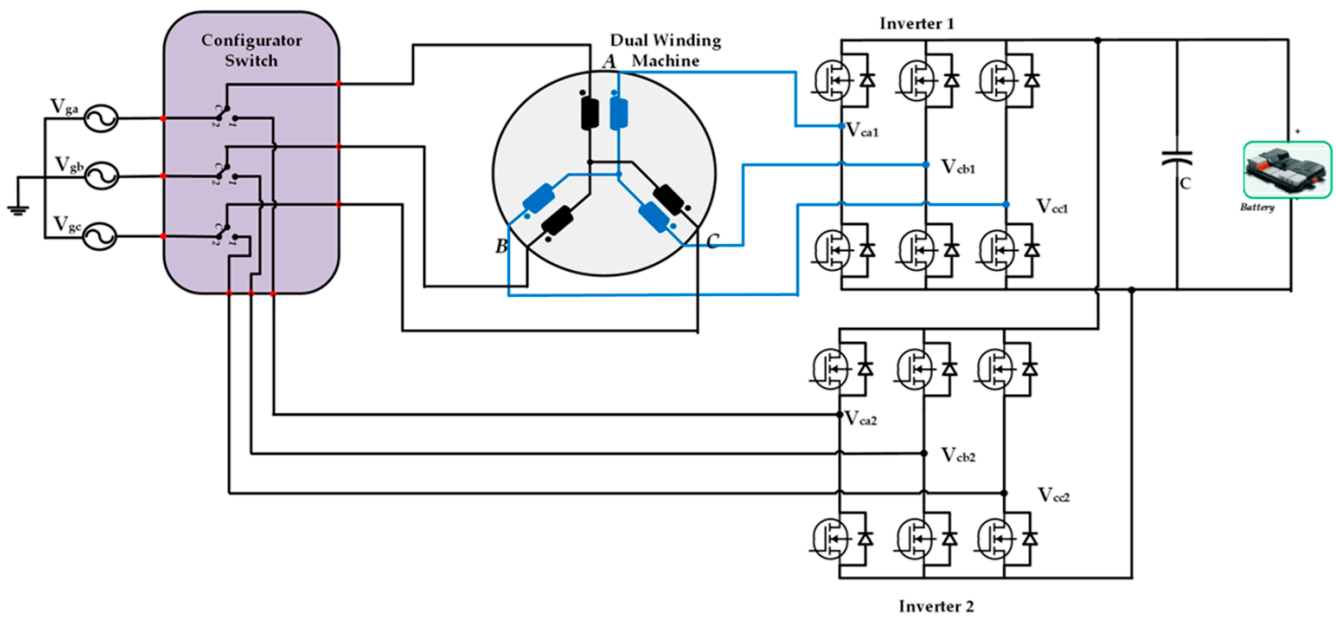


Figure 19. Isolated Integrated On-Board Charger based on Six Phase Machine Reconfiguration proposed by Pascetto et al. [94] in 2020 (iOBC15).

To sum up, we have seen the different aspects of the previously mentioned topologies, showing technical features such as V2G, torque ripple issues, and torque generation during charging. Thus, all topologies are compared according to the average torque production during the charging process, hardware reconfiguration between the propulsion and the charging modes, V2G feature, torque ripple issues, and the charging power as a ration of the traction power.

4. Control Techniques for iOBC

This section describes the charging and traction mode control techniques of motor drive integrated OBCs, including multiphase machines. There are many works is researching motor control techniques [95,96]. For this work, a detailed discussion of motor control strategies is not the focus. However, a brief discussion and comparison of the most common motor control approaches is included in Section 4.2. The battery charging mode control of an iOBC system as shown in Figure 20 is usually accomplished by two common techniques, constant current (CC) and constant voltage (CV).

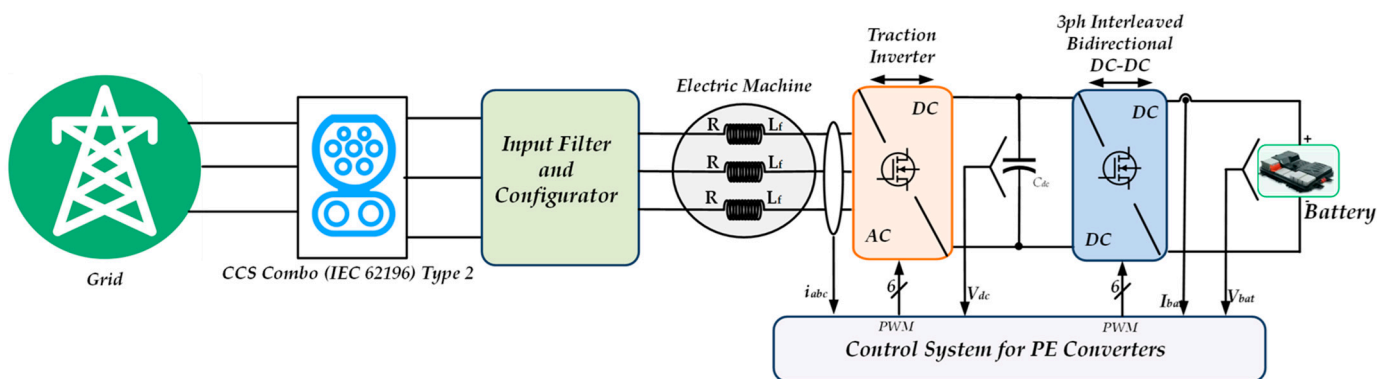


Figure 20. Integrated Power Converter with Control System in Charging Mode.

4.1. Charging Mode Controls for AC/DC Converter

Different battery charging methodologies have been adopted in the literature [97,98]. The integrated battery charging topology with CC, CV and CC-CV characteristics is shown

in Figure 21. We can select these control techniques based on the battery composition. The V2G/G2V control techniques (i.e., Hysteresis Current Control (HCC) [99], Proportional Integral (PI) control [100] and Proportional-Resonant (PR) control [101]) are used to achieve the power-flow control during the charging operating modes, according to the battery charging methodologies.

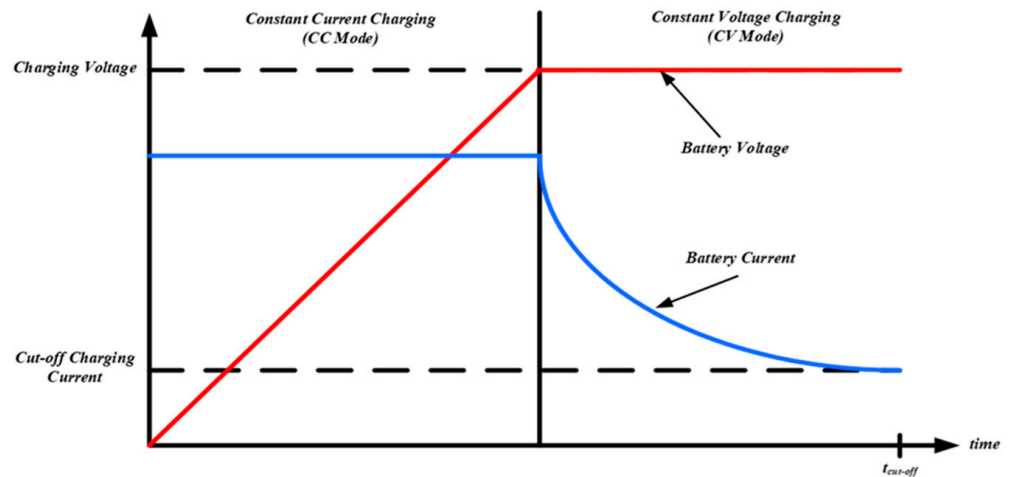


Figure 21. Constant-Current and Constant-Voltage (CC-CV) Charging.

4.1.1. Hysteresis Current Control (HCC)

The hysteresis current control works via an instantaneous feedback current control technique where the ac current follows the ac current within a hysteresis-band (Δh) [102]. This control strategy comprises two closed loops: outer voltage loop and inner current loop with HCC as shown in Figure 22. The outer voltage loop operates with the difference between actual and reference value of dc-link voltage. The PI control is used to achieve the desired voltage level. Moreover, the inner control loop does the same with sinusoidal ac currents. The HCC generates the switching pulses by ensuring that the ac currents follow the reference ac current i_a^* , i_b^* and i_c^* within the hysteresis band as shown in Figure 23. The main drawback of the HCC is that it has a variable switching frequency, which may lead to an increase in switching losses. Indeed, any time the current reference is not constant, the converter switching frequency will vary along the current reference period.

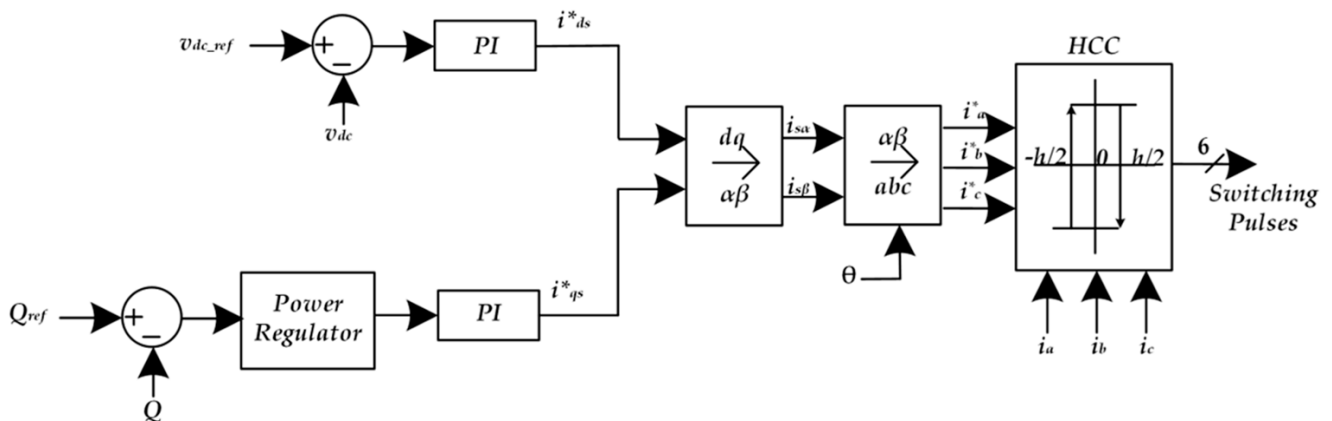


Figure 22. Hysteresis Current Control Strategy with two control loops.

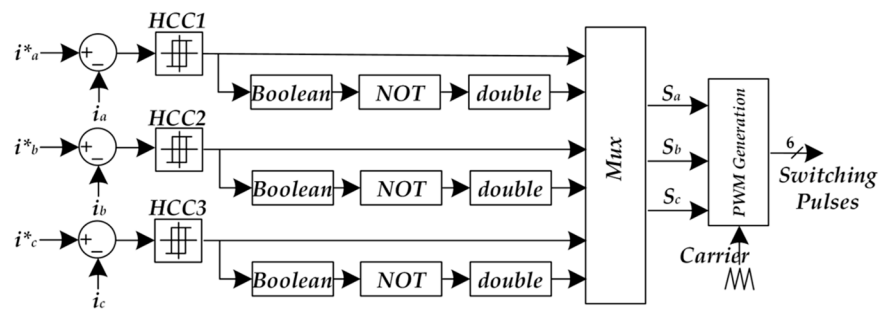


Figure 23. Switching Pulse Generation using hysteresis technique.

4.1.2. Proportional-Integral (PI) Based Dual Loop Control

The proportional-integral (PI) control solves the drawbacks of HCC. The PI can compensate for the current error and generates the control signals as shown in Figure 24. Then, this control signal v_{abc}^c is compared with the carrier signal to produce suitable switching patterns for the PE converter [100]. The phase locked loop (PLL) is used to determine the phase angle, θ , for inverse park transformation. The transfer function of the PI controller can be expressed as follows:

$$G_C(s) = K_p + \frac{K_i}{s} \tag{1}$$

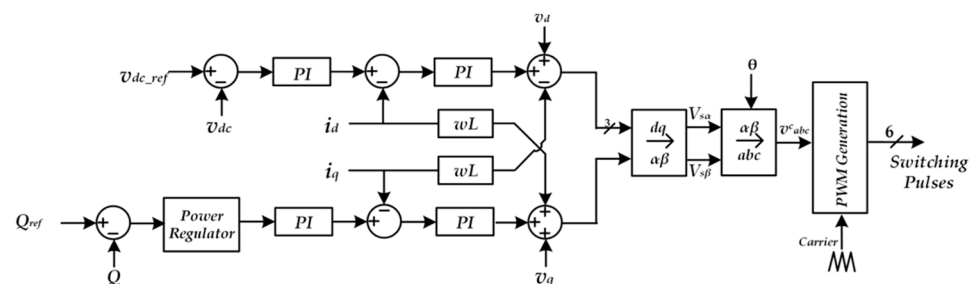


Figure 24. Proportional-Integral (PI) Control Strategy with dual control loop.

Here, K_p and K_i are the proportional and integral constants of the control loops, respectively.

4.1.3. Proportional-Resonant (PR) Based Dual Loop Control

The PR control methods are used to control the input current during charging/discharging modes. The PR is a well-known PI controller. However, the integral part is a generalized integrator in stationary frame [102]. The PR as shown in Figure 25 is more effective in stationary frame compared to the PI controller at achieving zero steady state errors. It also improves the reference tracking capability.

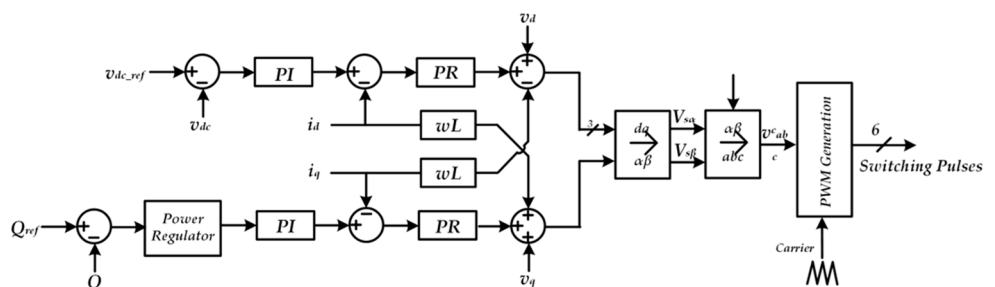


Figure 25. Proportional-Resonant (PR) Control Strategy with dual control loop.

In this control scheme, K_p determines the dynamic response of the control system, while K_i adjusts the phase shift between the output and the reference signals, and ω_0 is

the resonant frequency, which is set to $2\pi f$ (rad/s). f is the frequency of the ac grid. This shows the block diagram of the control system based on PR during the charging mode. The transfer function of the PR controller can be expressed as the equation

$$G_C(s) = K_{pi} + \frac{2K_i s}{s^2 + \omega_0^2} \tag{2}$$

4.1.4. Model Predictive Control (MPC)

Developments achieved over recent years in digital electronics, including digital signal controllers (DSCs), offer more computational power, potentiating the development of new and more effective and complex control techniques, such as the model predictive control (MPC) [103]. Figure 26 shows the MPC algorithm for performance of fast battery charging. This method is based on a predictive control method, which includes predicting the future behavior of the control variables and evaluating a cost function. Here, the cost function compares the reference value of a control variable with all possible predicted future values of a corresponding set of control variables.

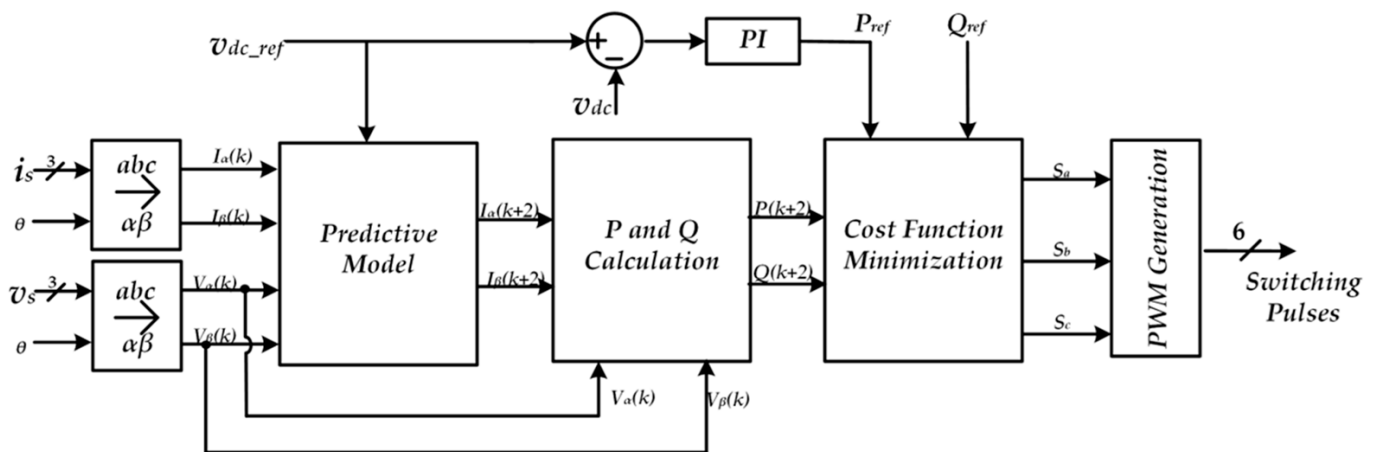


Figure 26. Model Predictive Control (MPC) Strategy for EV battery charging.

The input current prediction model can be derived using Euler Approximation of the power converter dynamic model expressed in the equation.

$$i_s(k + 1) = \left(1 - \frac{R_s T_s}{L_s}\right) i_s(k) + \frac{T_s}{L_s} [v_s(k) - v_{in}(k)] \tag{3}$$

Here, k represents the present time step whereas T_s is the sampling period. The grid voltage and current are denoted as i_s and v_s and the converter input voltage is v_{in} . The inductance and internal resistance value of the inductors are expressed as L_s and R_s . Using high sampling frequency approximation, we can obtain the cost function in this equation which is minimized over the prediction horizon.

$$v_s(k + 1) \approx v_s(k) \tag{4}$$

$$P(k + 1) \approx v_{s\alpha} i_{s\alpha} + v_{s\beta} i_{s\beta} \tag{5}$$

$$Q(k + 1) \approx v_{s\alpha} i_{s\alpha} - v_{s\beta} i_{s\beta} \tag{6}$$

$$g = |Q_{ref}(k) - Q(k + 1)| + |P_{ref}(k) - P(k + 1)| \tag{7}$$

Predictive control methods are appealing due to their advantages, such as a fast dynamic response, a simple structure that does not include a pulse width modulation block, and the ability to easily include constraints. This method has also benefitted from ongoing developments in high speed, cost-effective microprocessors [104,105].

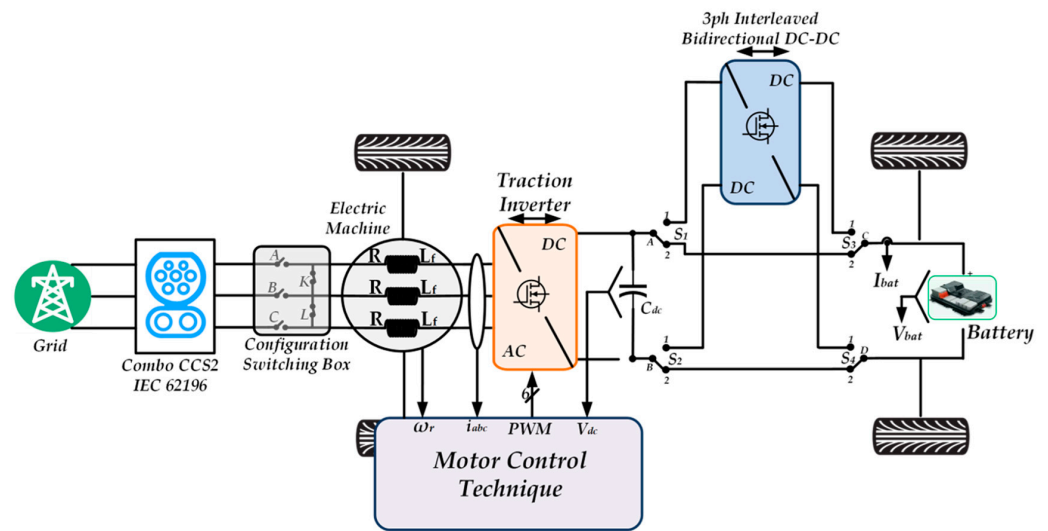


Figure 29. Motoring/Traction mode configuration of integrated on-board charger in EV.

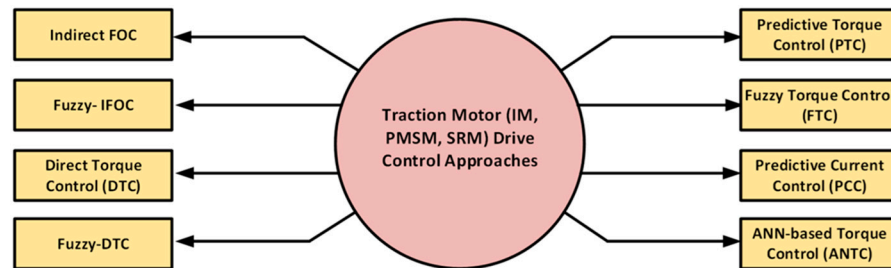


Figure 30. Various types of driving mode control used for integrated charging-traction system.

The performance qualities of different types of traction motor control strategies with a common load torque of 10 Nm are compared in Table 5.

Table 5. Performance comparison of different control strategies for traction motor control.

Features	IFOC	Fuzzy IFOC	DTC	FTC	PTC	PCC	ANNTC
References	[125–127]	[128,129]	[130–133]	[134]	[135]	[136–139]	[140]
Settling Time (ms)	200	50	250	250	250	400	40
Overshoot (%)	7	No Overshoot	6	9	9	13	3
Torque Response Time (ms)	200	50	250	250	250	400	40
EM Torque Ripple (%)	4	25	5	11	14	7	20
THD (%) of Flux	0.24	0.28	0.7	0.96	0.97	0.31	-
THD (%) of Current	0.56	1.16	7.35	7.21	9.34	1.56	-
Low Speed Performance	Excellent	Excellent	Poor	Poor	Poor	Poor	Good
Parameter Sensitivity	R_r and L_r	R_r and L_r	R_s	R_s	All Motor Parameters	All Motor Parameters	R_s

IFOC has the lowest torque ripple and THD in flux, contrasting with Fuzzy IFOC and DTC. In contrast, FTC and PTC use only one. PCC and PTC are the techniques with the most sensitive motor parameters, DTC and FTC being the most robust. IFOC, DIFOC and PCC use only current information, while DTC, FTC and PTC use torque and flux. Indeed, only one transformation is requested by the torque techniques, compared to the first three, which use two.

5. Comparative Analysis and Discussions

Table 6 shows the advantages, disadvantages and component counts among the traction inverter integrated on-board charging topologies with motor winding access, described in Section 3. All single-phase integrated charger topologies show that low THD during charging and low voltage and current ripple. Topologies such as iOBC3 and iOBC4 prove that there is no torque produced during the charging operation. However, the SRM

drive integrated on-board charger (iOBC6) needs a high component count, complex control and higher current THD. On the other hand, three phase topologies show common qualities like fast charging capability and good V2X performance. Topologies such as iOBC7 and iOBC8 use fewer passive components than others. The charging current THD is low for all the three phase topologies and efficiency is around 92%. Table 7 shows the features provided by the considered iOBC topologies including V2G, and the amount of THD during charging.

Table 6. Advantages and disadvantages of integrated on-board charger topologies.

Reference	Advantages	Disadvantages	Components
[61]	<ul style="list-style-type: none"> • Low output filter inductor and capacitor size • Lower switching voltage stress • Good PF performance. 	<ul style="list-style-type: none"> • Poor current THD in higher voltage operation • Complex control method • V2G feature is not possible 	<ul style="list-style-type: none"> • 10 IGBT Switches • 10 Diodes • 1 Inductors • 3 Capacitors
[62]	<ul style="list-style-type: none"> • Low output current ripple • Easy control method • Low THD • High Efficiency 	<ul style="list-style-type: none"> • Size and Weight is high due to higher additional boost inductor • Additional Hardware needed 	<ul style="list-style-type: none"> • 14 IGBT Switches • 16 Diodes • 3 Inductors • 2 Capacitors • 2 Relays
[64]	<ul style="list-style-type: none"> • Fast charging • V2G feature • THD is low • Torque free operation during charging/V2G 	<ul style="list-style-type: none"> • 4 Motor used • Complex traction control • High component count • High power battery needed 	<ul style="list-style-type: none"> • 24 IGBT Switches • 24 Diodes • 1 Inductors • 1 Capacitors
[66]	<ul style="list-style-type: none"> • Torque free operation during charging • Simple control strategy • Unity PF operation • Low charging current ripple 	<ul style="list-style-type: none"> • Slow charging time • High torque ripple • Efficiency is low • High voltage ripple • Additional hardware needed 	<ul style="list-style-type: none"> • 6 IGBT Switches • 6 Diodes • 1 Inductors • 2 Capacitors • 4 Relay Switches
[67]	<ul style="list-style-type: none"> • Low voltage stress on switch • Standard motor drive configuration • High efficiency at higher voltage 	<ul style="list-style-type: none"> • High charging current ripple • Size of heatsink is big • Extra control needed for relay coordination 	<ul style="list-style-type: none"> • 6 IGBT Switches • 6 Diodes • 1 Capacitor • 2 DP Relay Switches • 3 SP Relay Switches
[68]	<ul style="list-style-type: none"> • Good traction performance • Good filter design • Low voltage and current ripple • V2X performance is good 	<ul style="list-style-type: none"> • High component count • Complex control strategy • Higher current THD • High system cost 	<ul style="list-style-type: none"> • 12 IGBT Switches • 14 Diodes • 2 NPN Transistors • 5 Capacitors • 4 Inductors • 2 DP Relay Switches • 3 Magnetic Contactors
[68]	<ul style="list-style-type: none"> • Fast charging • No modification needed • Simple Control • High Efficiency, Low THD 	<ul style="list-style-type: none"> • High inverter loss • High noise • V2G feature is not possible 	<ul style="list-style-type: none"> • 6 IGBT Switches • 3 SiC Switch Interface • 21 Diodes • 1 Capacitors
[73]	<ul style="list-style-type: none"> • Low harmonic content during charging • Low current ripple • Low THD in charging current 	<ul style="list-style-type: none"> • Machine rewinding is required • V2G operation is not efficient. • Torque ripple is high 	<ul style="list-style-type: none"> • 14 IGBT Switches • 14 Diodes • 1 Inductors • 1 Capacitors
[87]	<ul style="list-style-type: none"> • Torque free charging. • Low THD (2.7%) during driving • No torque ripples • AC and DC charging is compatible 	<ul style="list-style-type: none"> • Control method is complex. • Efficiency is low • High power performance is poor 	<ul style="list-style-type: none"> • 18 IGBT Switches • 24 Diodes • 4 Capacitors
[88]	<ul style="list-style-type: none"> • Compatible with multiphase machine • Low switch count used for charging and driving • High power performance is good • Torque free charging 	<ul style="list-style-type: none"> • Additional switches are needed for configuration • Low voltage utilization factor • High current ripples • Poor charging current THD 	<ul style="list-style-type: none"> • 11 IGBT Switches • 11 Diodes • 1 Inductors • 1 Capacitors • 3 Magnetic Contactors

Table 7. Feature comparison of integrated on-board charger topologies.

Topology	No of Machine Phase	Type of Supply	No of HBM Inv	Hardware Config. Needed	Charging with Zero Torque	Traction Power	Charging to Traction Power Ratio	V2G Feature	Torque Ripple Issue
[61]	3	1ph	5	No	Yes	>8 kW	25%	No	Yes
[62]	3	1ph	6	No	Yes	>3.3 kW	100%	Yes	No
[64]	3	1ph	12	No	Yes	>7 kW	100%	Yes	No
[66]	3	1ph/3ph	3	Yes	Yes	>15 kW	30%	Yes	No
[67]	3	1ph	3	Yes	Yes	>6 kW	50%	No	No
[68]	3	1ph	3	Yes	Yes	>5 kW	100%	No	Yes
[70]	3	3ph	6	No	Yes	>6.6 kW	50%	No	No
[71]	3	1ph/3ph	6	No	Yes	>30 kW	75%	Yes	Yes
[83]	3ph-9Seg	3ph	9	No	Yes	>5.5 kW	100%	Yes	No
[82]	3ph-6Seg	3ph	6	No	Yes	>6.6 kW	100%	No	No
[68]	3	1ph/3ph	3	Yes	Yes	>22 kW	100%	Yes	No
[73]	9	1ph/3ph	9	Yes	Yes	-	-	Yes	Yes
[87]	6	1ph/3ph	6	Yes	Yes	>3.3 kW	100%	Yes	No
[88]	5	1ph/3ph	5	Yes	Yes	>4 kW	60%	Yes	Yes

The qualitative analysis of the motor drive integrated on-board charger is explained by nightingale rose diagram in Figure 31. As described in an earlier section, iOBC1–iOBC9 represent the single-phase topologies and the rest are three phase topologies. From the figure, it is observed that the three phase topologies from iOBC12 to iOBC15 have multifunctional ability with an average 12–18 total component count. However, the control strategies they use are complex compared to the single-phase topologies.

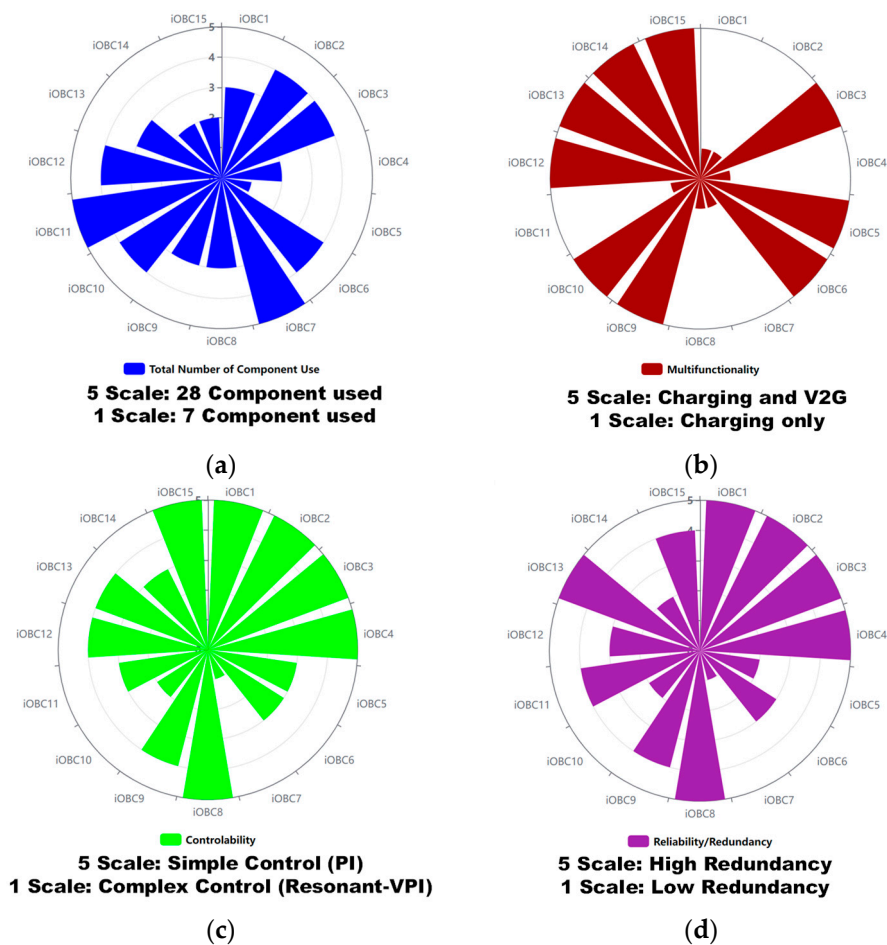


Figure 31. Cont.

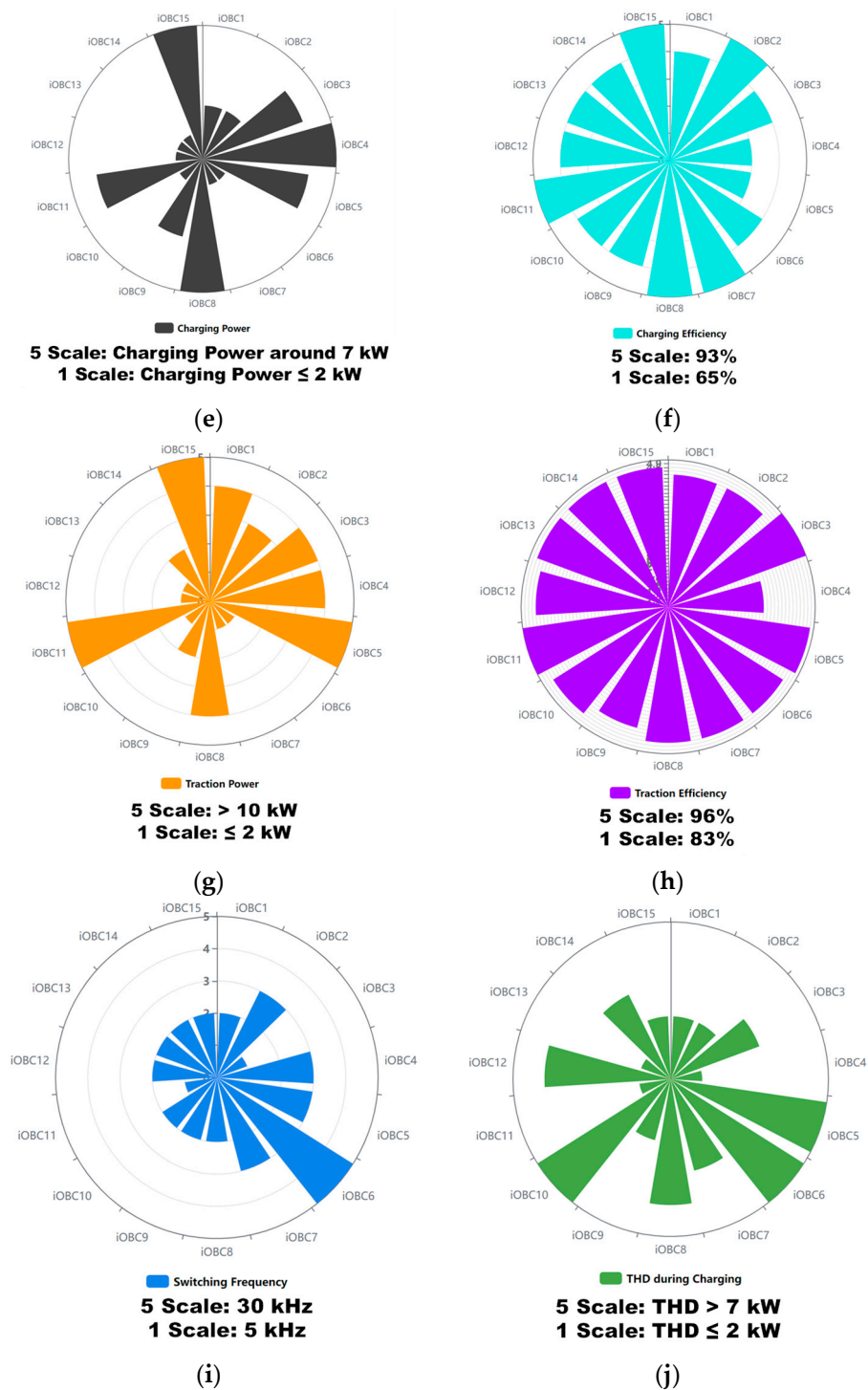


Figure 31. Qualitative analysis of iOBC topologies, (a) Total number of components used, (b) V2G Capability, (c) Controllability, (d) Reliability/Redundancy, (e) Charging power, (f) Charging efficiency, (g) Traction power, (h) Traction efficiency, (i) Switching frequency, (j) THD during charging.

The simple PI control is used in most of the single-phase topologies. Additionally, the reliability or redundancy is high compared to the three phase topologies. The charging and traction efficiency for all topologies is between 85–95%, though the experimental setup for validation of the simulation is not very high. The maximum charging power tested is around 7 kW whereas the traction power is around 10 kW for all the topologies. The topologies iOBC4, iOBC8 and iOBC15 are tested at around 7 kW charging power. On the

other hand, almost all topologies are tested at around 10 kHz switching frequency except iOBC6, which operates at 30 kHz, as illustrated in Figure 32.

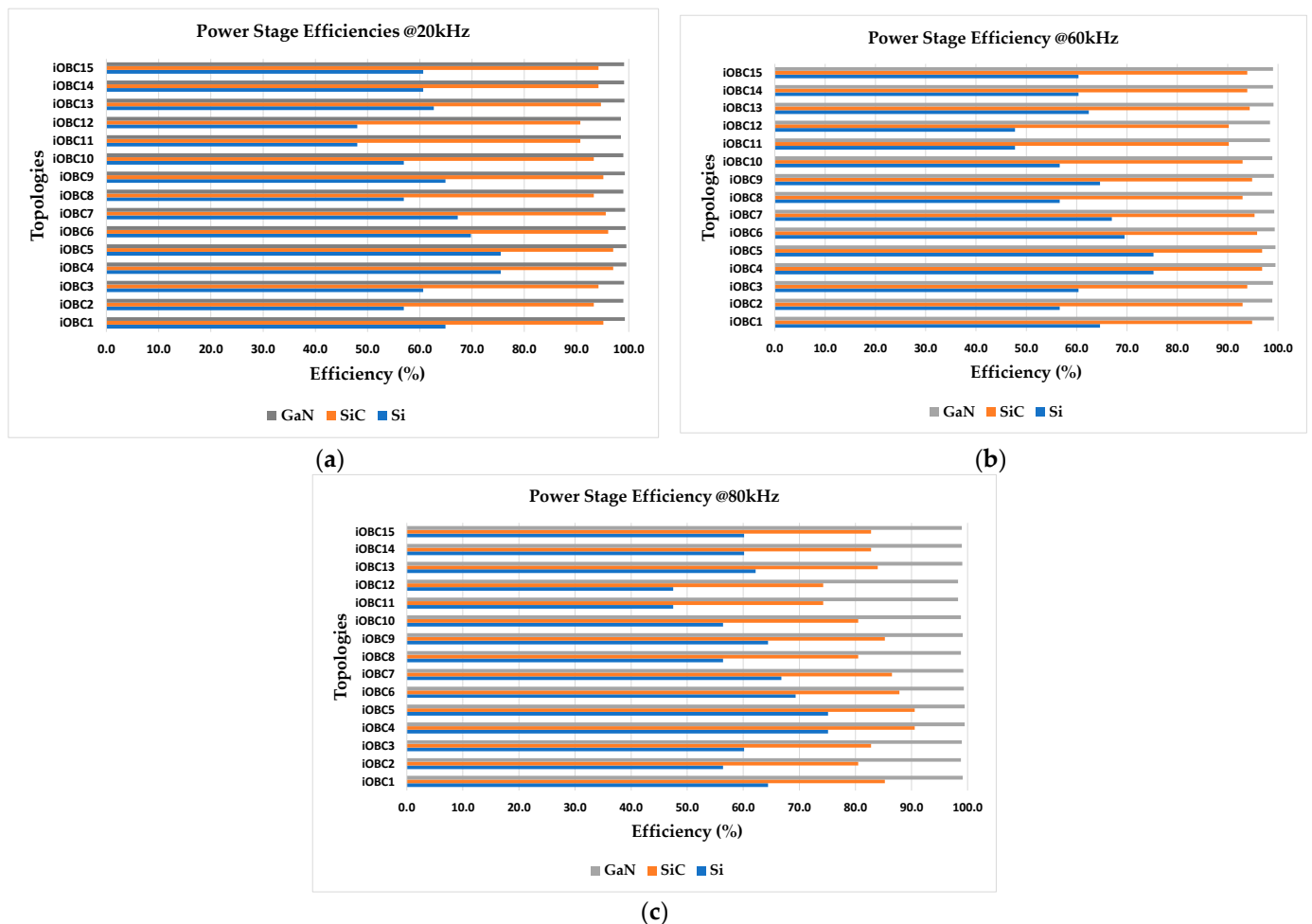


Figure 32. Estimated efficiencies for all considered iOBC power stages with different switching technologies. (a) 20 kHz, (b) 60 kHz, (c) 80 kHz.

However, iOBC6 shows a high THD value during the charging operation. Conversely, the three phase topologies show a THD value of less than 5%, which ensures good charging power quality. On the other hand, it is shown in the topology section that the iOBC topologies use a high power traction inverter and DC-DC converter during charging. Thus, level 3 AC fast charging (up to 43.5 kW with 400 VAC) is possible to charge the EV. In this context, the converter losses and efficiencies for all the topologies are also investigated at different switching frequencies. For all considered topologies, the efficiency is estimated up to a 44 kW system for 400 VAC charging input and 250 V minimum battery voltage during charging. It is important to mention that only a power stage with an active semiconductor switch is considered for the efficiency calculation. The passive elements, relays, etc., are not considered. It is clearly visible that all single-phase topologies show poor efficiency for the Si IGBT switch, which is less than 70%, whereas SiC and GaN switch technology displays above 95% efficiency. For three-phase integrated OBC power stages, SiC technology shows around 92% efficiency up to 60 kHz, compared to Si technology which is below 70%, though the efficiencies are slightly less at 80 kHz. The GaN switch technology is a highly efficient switch overall for design of a 44 kW system. However, it requires a very good gate drive circuit with different kinds of protection mechanism.

6. Electric Vehicle Charging Standards

A group of experts have created international standards which are widely accepted. Various worldwide standards are being established and published to successfully deploy EV chargers. These have been thoroughly designed to address the EV industry's safety, reliability, and interoperability concerns. EV and ESS manufacturers, utility companies, EV charger manufacturers, code authorities, EV charger safety equipment makers, and insurance organizations are among the businesses that use these standards.

Different EV charging standards [37,141–145] in the literature are discussed in Table 8.

Table 8. International standards for electric vehicle charging stations.

Standard Code	Descriptions	Standard Authority
General EV Charging and Maintenance Standards [37,141]		
J1772	EV conductive charging connector standard (Type1). The SAE J1772-2017 standard defines four levels of charging: AC Level 1, AC Level 2, DC Level 1, and DC Level 2	SAE ¹
J1773	EV inductive coupled charging standard for AC Level 1, 2 and 3. This type of inductively coupled charging is generally intended for transferring power at frequencies significantly higher than power line frequencies.	SAE ¹
J2293	Energy transfer requirements from power utility to EV through the EVSE. This document defines, either directly or by reference, all characteristics of the total EV Energy Transfer System (EV-ETS) necessary to insure the functional interoperability of an EV and EVSE of the same physical system architecture.	SAE ¹
NEC 625/626	Electric vehicle charging and supply equipment system requirements	NFPA ⁴
NFPA 70E	Safety standards for employees who work on or near exposed energized electrical conductors or circuit parts	NFPA ⁴
NFPA 70B	Recommended practice for electrical equipment maintenance	NFPA ⁴
IEEE 2030.1.1	This standard specifies the design interface of electric vehicles and direct current (dc) quick chargers that promote interoperability and rapid charging of electric vehicle. A communication method used for transmitting control signals between an electric vehicle and a quick charger in the CHAdeMO system. (ISO 11898-2)	IEEE ³
IEEE P1809	Sustainable electric vehicle guide.	IEEE ³
IEC TC 69	EVs infrastructure safety, electrical installation, electric shock protection	IEC ²
G101-109	Fast charging station operation and communication standards.	JEVS ⁷
Power Quality Standards [141,142]		
J2894	The intent of this document is to develop a recommended practice for PEV chargers, whether on-board or off-board the vehicle, that will enable equipment manufacturers, vehicle manufacturers, electric utilities, and others to make reasonable design decisions regarding power quality. According to this document, the power quality requirements for Plug-In Vehicle chargers are shown <10%).	SAE ¹
IEEE 519-2014	This defines the voltage and current harmonics distortion criteria for the design of electrical systems (THD < 8%). The standard adopts the 10/12 cycles gapless harmonic subgroup measurement from the IEC 61000-4-7. Aggregations of 150/180 cycles (~3 s) and 10 min are required for the statistical assessments.	IEEE ³
IEC-1000-3-6	According to this standard, the current limits are more case and system dependent, which is supposed to result in fewer restrictions to customers. However, the calculation of current limits relies on many assumptions; these assumptions could defeat the good intentions of the ZEC standard. The EMC requirements for power supplied in Europe. (THD < 8% in low and medium voltage)	IEC ²
GB/T 14549	Harmonics requirements for power supplied in China (THD < 5% for low voltage)	GB ⁸
Charging Station Management Standards [141]		
NFPA 70	Safety management for electric vehicle charging station	NFPA ⁴
IEC TC 21	Recommendation for EV energy storage system management	IEC ²

Table 8. Cont.

Standard Code	Descriptions	Standard Authority
EVSE Communication Standards [141,146]		
J2836/J2847/J2931	This document applies to the off-board DC charger for conductive charging, which supplies DC current to the Rechargeable Energy Storage System (RESS) of the electric vehicle through a SAE J1772™ coupler. Communications will be on the SAE J1772 Pilot line for PLC communication. The details of PowerLine Communications (PLC) are found in SAE J2931/4.	SAE ¹
IEEE 1901	Provide data rate while vehicles are charged overnight	IEEE ³
IEEE P2690	Charging network management, Vehicle Authorization	IEEE ³
ISO 15118-1	Road vehicles—Communication protocol between electric vehicle and grid—Part 1: Definitions and use-case	ISO ⁶
ISO 15118-2	Road vehicles—Communication protocol between electric vehicle and grid—Part 2: Sequence diagrams and communication layers. The purpose of ISO 15118-2:2014 is to detail the communication between an EV (BEV or a PHEV) and an EVSE. Aspects are specified to detect a vehicle in a communication network and enable an Internet Protocol (IP) based communication between EVCC and SECC.	ISO ⁶
V2X Standards [141,143]		
IEEE 1547	Standards for interconnection between grid and distributed energy sources	IEEE ³
IEEE P2030	Interoperability of EV charging station and microgrid	IEEE ³
UL 1741	Standard for Inverters, Converters, Controllers and Interconnection System Equipment for use with Distributed Energy Resources	UL ⁵
EV Charging Station Protection and Safety Standards [143–145]		
UL 2594/2251, UL 2201/UL 2231	Safety requirements for EV OBC system supplied by a branch circuit of up to 600 V for recharging the battery	UL ⁵
UL 225a	Recommendation related to the rules of protection regarding couplers, plugs, and receptacles	UL ⁵
ISO 6469	Safety recommendation for personal protection and EV storage system	ISO ⁶
IEC 60950	Safety requirements of technology equipment's for the voltage level lower than 600 V	IEC ²
IEC TC 64	EVs infrastructure safety, electrical installation, electric shock protection	IEC ²
ISO 6469-1:2009	Electrically propelled road vehicles—Safety specifications—Part 1: Onboard rechargeable energy storage system (RESS)	ISO ⁶
ISO 6469-2:2009	Electrically propelled road vehicles—Safety specifications—Part 2: Vehicle operational safety means and protection against failures	ISO ⁶
ISO 6469-3:2009	Electric road vehicles—Safety specifications Part 3: Protection of persons against electric hazards	ISO ⁶
J2910	This standard deals with the electrical safety of buses and test for hybrid electric trucks	SAE ¹
J2344	Recommendation for EV safety rules	SAE ¹
J2464	Electric and Hybrid Electric Vehicle Rechargeable Energy Storage System (RESS) Safety and Abuse Testing	SAE ¹
DIN V VDE 0510-11:	Safety requirements for secondary batteries and battery installations—Part 11: Safety requirements for secondary lithium batteries for hybrid vehicles a mobile application	VDE ⁹

¹ SAE: Society of Automotive Engineers; ² IEC: International Electromechanical Commission; ³ IEEE: Institute of Electrical and Electronic Engineers; ⁴ NFPA: National Fire Protection Association; ⁵ UL: Underwriters Laboratories Inc; ⁶ ISO: International Organization of Standardization; ⁷ JEVS: Japan Electric Vehicle Standard; ⁸ GB/T: Guojia Biaozhun/Tujian (China); ⁹ VDE: Verband Deutscher Elektrotechniker (Germany).

7. Integrated On-Board Charger Power Density SoTA

It is clear from the review study that the technology now on the market or in development is not mature or versatile enough to allow for such integration in vehicle development. Power electronics converters in BEV and PHEV powertrains, for example, are mostly made of Si-based semiconductors. The efficiency of these converters is limited to 92–93%, the switching frequency is limited to 30 kHz, and a power density of just 0.18–0.73 W/L is achievable. Therefore, WBG materials are quickly becoming the mainstay of integrated power electronics converters. SiC and GaN are quickly becoming commercially viable alternatives to Si as the material to construct future integrated iOBCs. Figure 33 depicts the current state of the art for integrated motor drives, with power densities in kW/L and

kW/kg [96,147–153]. The power density for commercial integrated motor drive ranges from a minimum of 2.4 kW/L (Nissan Leaf) in 2012 to a maximum of 15.3 kW/kg (Bosch Gen3) in 2019, whereas the majority of electric vehicles on the market in 2021 use Si semiconductors (such as the VW ID.3 with the new Infineon HybridPACK™ drive).

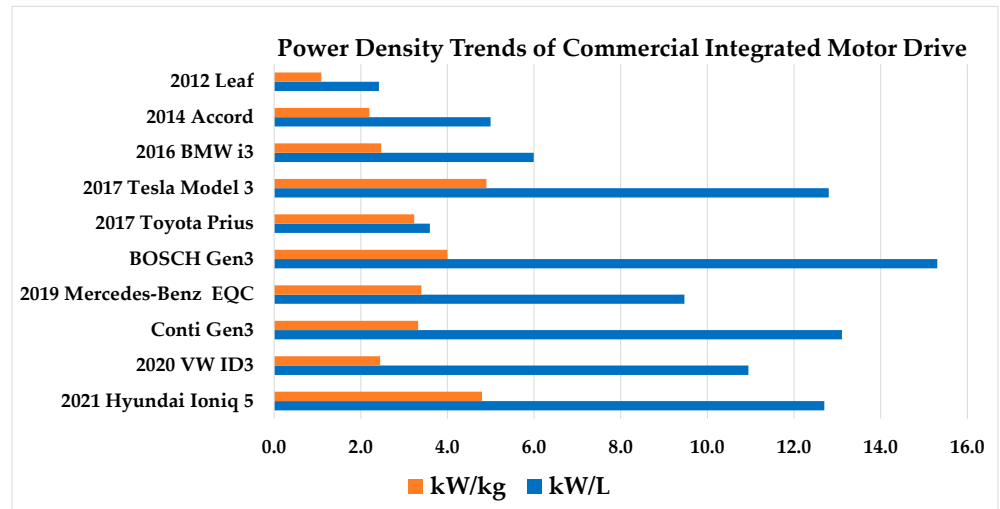


Figure 33. Estimated power density state of the art of commercially available integrated motor drive.

In contrast, the giant EV manufacturers like Tesla and Hyundai have already planned to use SiC technology in power electronic systems for their recent models such as Hyundai IONIQ 5 (released in April 2021). Although the volumetric density of the Tesla Model 3 is the highest among all commercial motor drive iOBCs listed here, there is a relatively high galvanometric density of 4.5 kW/kg due to the usage of SiC technology. Finally, the estimated maximum power densities for the combination of inverter and on-board charger are 14.8 kW/L and 12.3 kW/kg for Hyundai IONIQ 5 (launched in April 2021) which is shown in Figure 34. However, the volumetric densities overview is incomplete; not all data is accessible for an approximate computation.

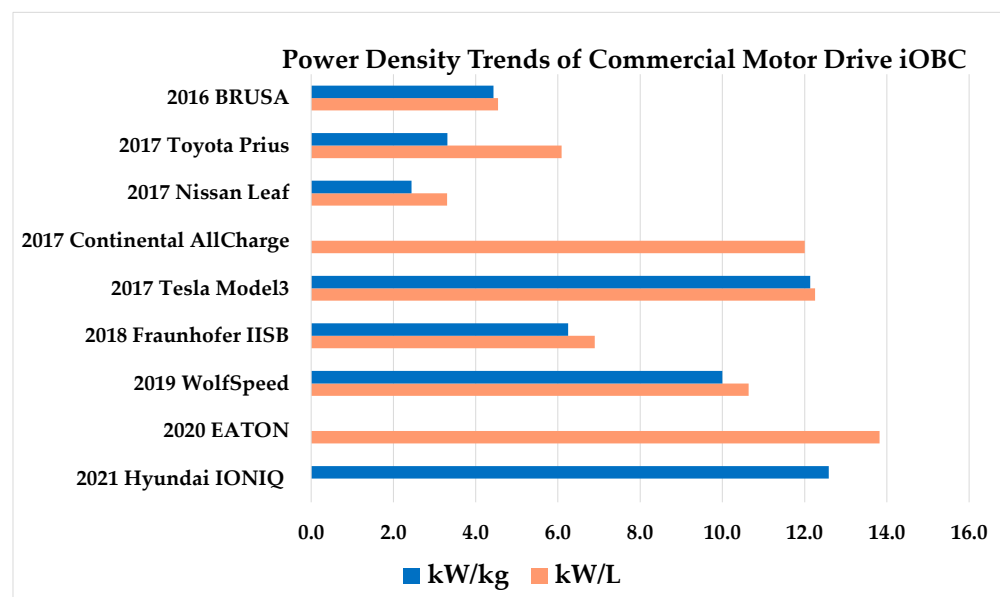


Figure 34. Estimated power density state of the art for commercially available integrated on-board chargers (iOBC).

The technology currently on the market or in development is not mature and not flexible enough to enable such an easy integration in vehicle development. For instance, the power electronics converters used in BEV and PHEV powertrains primarily use Si-based semiconductors. These converters are limited in several ways: the efficiency is limited to 92–93%, switching frequency cannot go above 30 kHz and power densities of only 0.18–0.73 W/L are attainable. The WBG semiconductors have brought drastic improvements in power density and efficiency. Some giant car manufacturers such as Hyundai, Tesla, and Volkswagen are using an advanced WBG switch pack to increase the power density of the power converters. The linear power density trendline with collected data shows that the projected volumetric and galvanometric power density touches at approximately 25 kW/L and 20 kW/kg in 2025, which is depicted in Figure 35. The power density trend of iOBC with a DC/DC converter is illustrated in Figure 36.

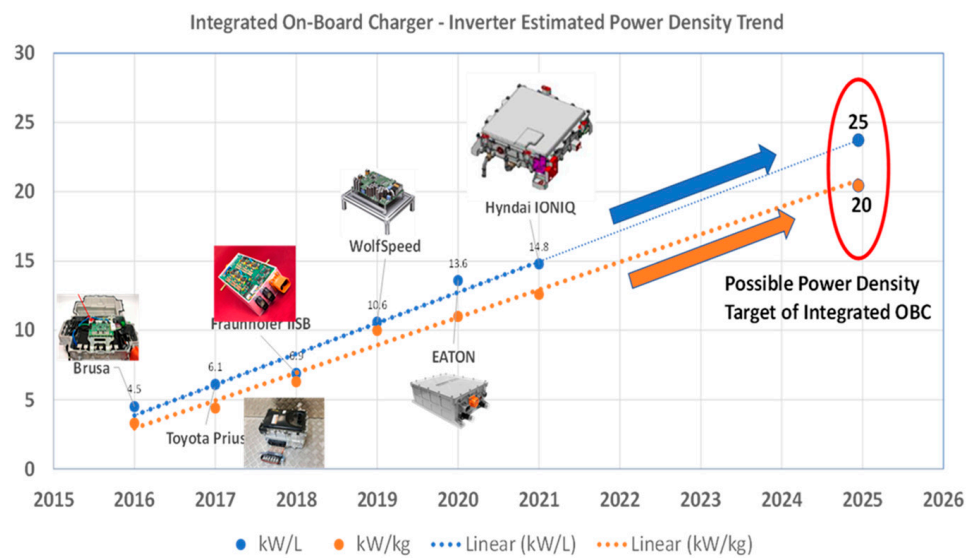


Figure 35. Estimated power density trend of integrated on-board charger (iOBC) with motor drive.

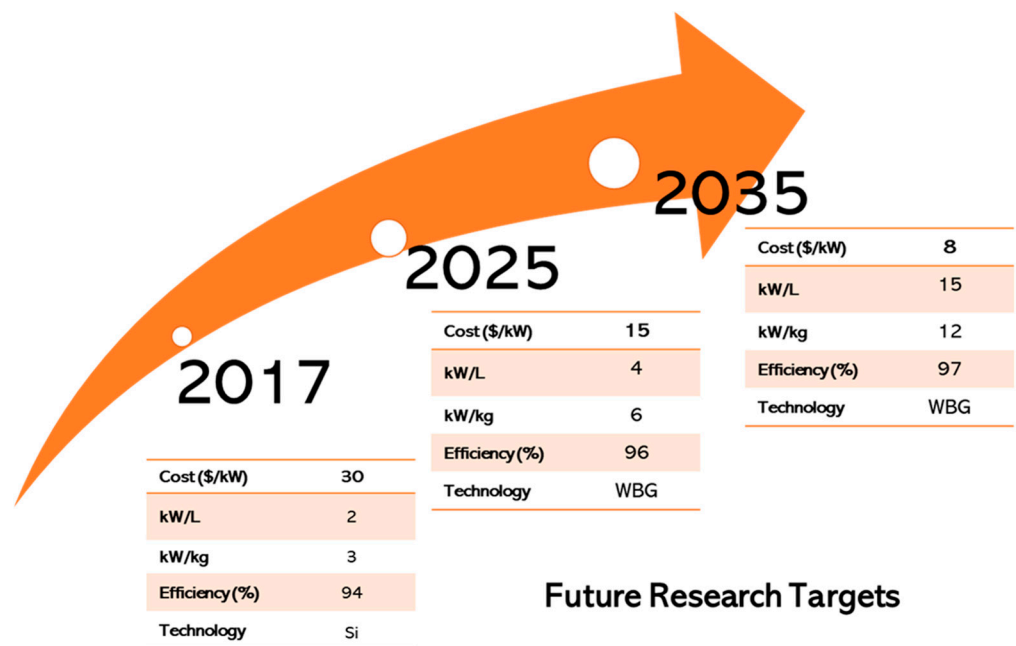


Figure 36. Estimated power density trend of integrated on-board charger (iOBC) with DC/DC converters.

The bibliometric analysis is performed on an integrated on-board EV charger in Scopus. The base parameter of the analysis is the number of published documents such as journals, conference proceedings, book chapters, etc. We performed this bibliometric study from 2010 until 2022. The documents published by different affiliations, authors, and publication sources are depicted in the following Figures 37–40.

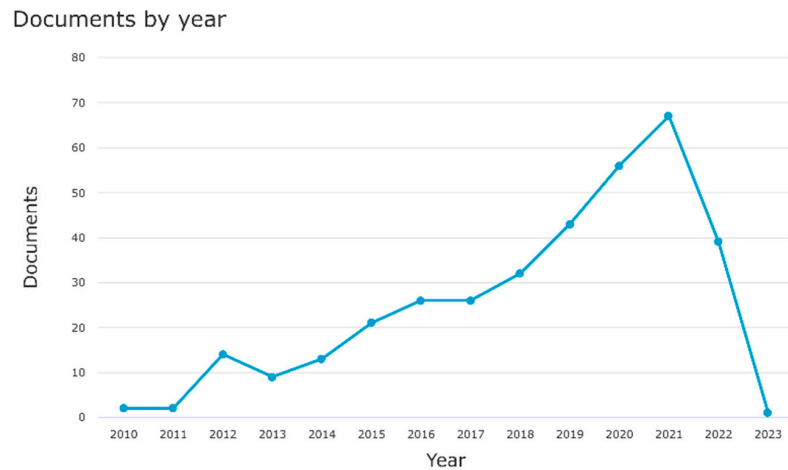


Figure 37. Publication per year on iOBC for electric vehicles from 2010 to until 2022.

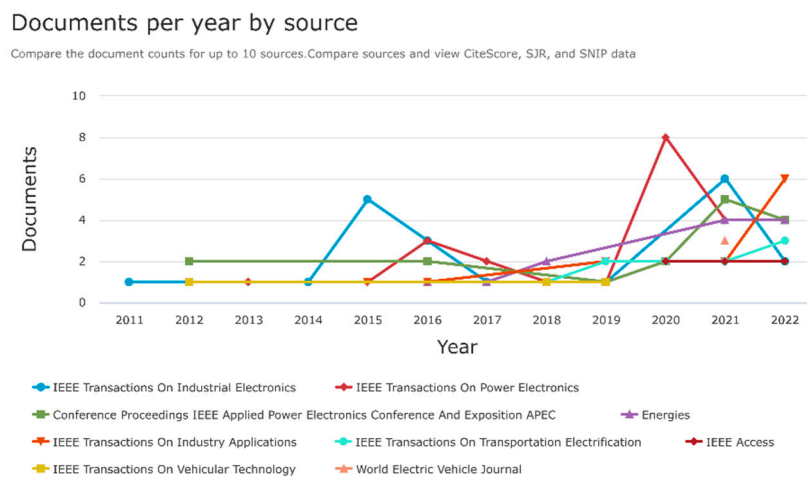


Figure 38. Publication per year by different publishers from 2020 to 2022.

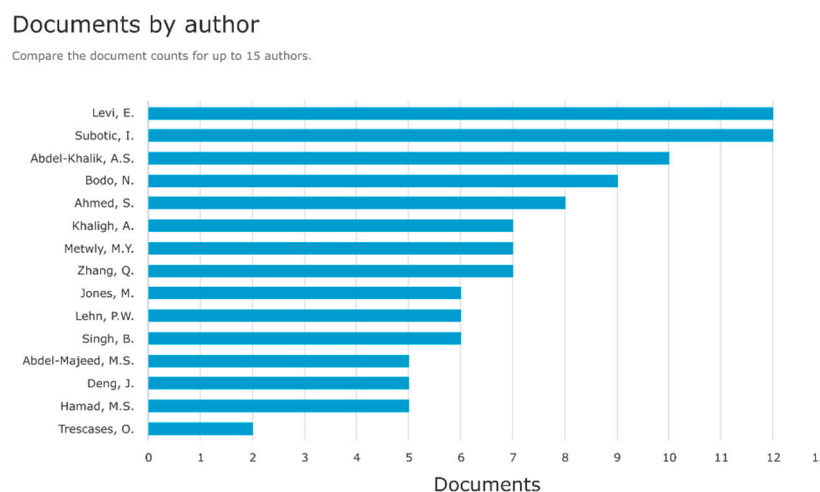


Figure 39. Publication status of top 15 authors on iOBC for electric vehicles from 2010 to until 2022.

Documents by affiliation

Compare the document counts for up to 15 affiliations.

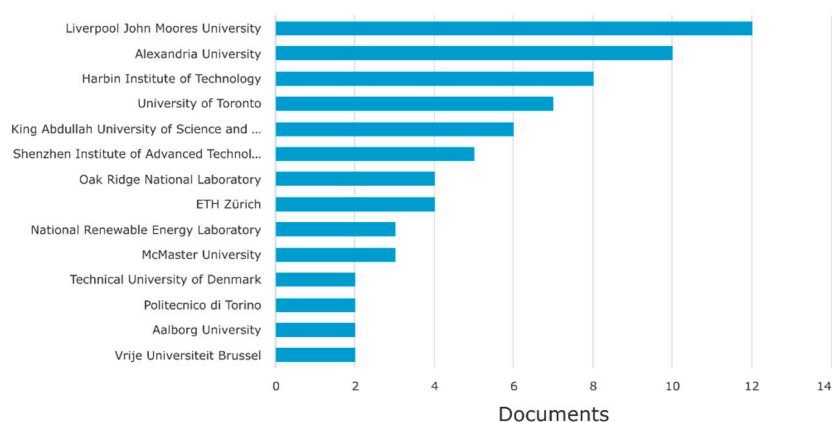


Figure 40. Publication status of top 15 higher educational institutions for iOBC for electric vehicles from 2010 to until 2022.

8. Economic and Environmental Impact of iOBC

Increasing usages of iOBC will reduce the total number of required converters in EV drivetrains. From a conventional EV structure, iOBC will reduce utilization of the two power electronics converter (i.e., AC/DC and isolated DC/DC). Thus, the required carbon-footprint to produce a commercial passenger car will reduce in those vehicles where iOBC is employed due to reducing usages of semiconductors (i.e., Si, SiC or GaN) and magnetic materials. Fewer components on EVs will accelerate the shift to zero-tailpipe emission solutions and environmentally friendly mobility, also resulting in cleaner air in cities and thus a higher quality of life for citizens.

The economic impact of iOBC is also significant. The following impact is determined via brainstorming:

- The implementation of iOBC solution will strengthen the competitiveness of EU companies, particularly the OEMs which can benefit from the commercialization of developments.
- The car manufacturers will be able to increase their turnover due to sales of innovative products, subsequently enhancing their positioning in the EV worldwide market by using innovative iOBC solutions.
- The component level OEMs will be able to sell new services related to their testing business, also enhancing their infrastructure and labs for unique positioning of novel bidirectional testing activities.
- This increase in competitiveness will be translated into maintaining jobs and expertise in Europe.
- Impact of modular, flexible and bi-directional iOBC systems in increasing EVs adoption
 - ✓ Improved charging procedures without increasing battery size/price
 - ✓ Improved user-friendliness and contribution to meeting end-user expectations
 - ✓ Reduce costs on infrastructure side
 - ✓ Generate new opportunities for the user
 - ✓ Impact on time to market and accelerated adoption
- Proven scalability and functionality with different vehicle brands and different vehicle segments presented in the state-of-the-art review of iOBC topologies for BEV and PHEV powertrains, including control.

9. Conclusions

This paper presented a state-of-the-art review of iOBC topologies for BEV and PHEV powertrains, including control approaches and industrial power density trends. This

review focuses on multiple performance features, such as multifunctionality, controllability, charging current THD, voltage and current ripples, charging and traction efficiencies, which directly influence the selection of a particular iOBC structure for respective BEV and PHEV powertrains. This paper also shows possible integration approaches for an OBC with other power electronics modules. It can be seen from this review that the iOBC9 is a good option for a non-isolated iOBC structure. However, there is a need for isolation between the grid and battery during charging.

To conclude, the iOBC15 is the best option for mainly low-power BEVs and PHEVs, having excellent charging power quality, moderate cost, compact size and volume. On the other hand, the iOBC7 and iOBC8 are suitable for high-power BEVs and PHEVs, as all have low switching losses, high efficiency, and simple controllability. In the case of battery charging control approaches, the proportional-resonant control is the most favored option due to its linear correlation, small overshoot, and high sensitivity for high power applications. In the case of the motor control, the Hybrid IFOC with MPC depicts a better response due to its high efficiency, simple control technique and design process. However, IFOC has a positive impact on the switching devices rather than MPC, in terms of reliability assessment. Finally, with the power density trends of integrated technologies, Hyundai IONIQ 5, which was released in April 2021, designed a motor drive integrated OBC with higher volumetric density compared to the previous state-of-the-art solutions, whereas the Tesla Model 3 has an iOBC with around 12 kW/L. Both use SiC technology. On the other hand, the galvanometric density of Hyundai IONIQ 5 is slightly higher compared to Tesla Model 3, which is around 12 kW/kg. Therefore, future integrated OBC design can consider these car manufacturers' design and recent state of the art developments for further improvement.

Funding: This project has received funding from the European Union's Horizon 2020 research and innovation program under grant agreement 875131 (eCharge4Driver).

Institutional Review Board Statement: Not applicable.

Informed Consent Statement: Not applicable.

Data Availability Statement: Not applicable.

Acknowledgments: The authors would like to acknowledge the eCharge4Driver project partners. Authors also acknowledge the Flanders Make for their support to the MOBI-EPOWERS research group.

Conflicts of Interest: The authors declare no conflict of interest.

Abbreviations

AFE	Active Front-End
ANN	Artificial Neural Network
ANNTC	Artificial Neural Network based Torque Control
BEV	Battery Electric Vehicle
CC	Constant Current
CM	Common Mode
CV	Constant Voltage
DSC	Digital Signal Controller
DTC	Direct Torque Control
EMI	Electromagnetic Interference
EV	Electric Vehicle
FL	Fuzzy Logic
FTC	Fuzzy based Torque Control
G2V	Grid-to-Vehicle
GaN	Galium Nitride
GB/T	Guojia Biaozhun/Tuijian (China)

HCC	Hyteresis Current Control
ICE	Internal Combustion Engine
IEC	International Electromechanical Commission
IEEE	Institute of Electrical and Electronic Engineers
IFOC	Indirect Field Oriented Control
IM	Induction Machine
iOBC	Integrated On-board Charger
ISO	International Organization of Standardization
JEVS	Japan Electric Vehicle Standard
MPC	Model Predictive Control
NFPA	National Fire Protection Association
OEM	Original Equipment Manufacturer
OEWM	Open-End Winding Machine
PCC	Predictive Current Control
PEV	Plug-in Electric Vehicle
PI	Proportional Integral
OEM	Original Equipment Manufacturer
OEWM	Open-End Winding Machine
PCC	Predictive Current Control
PEV	Plug-in Electric Vehicle
PI	Proportional Integral
PLL	Phase Locked Loop
PMSM	Permanent Magnet Synchronous Machine
PR	Proportional Resonant
PTC	Predictive Torque Control
SAE	Society of Automotive Engineers
SiC	Silicon Carbide
SRM	Synchronous Reluctance Machine
T1FLC	Type 1 Fuzzy Logic Control
T2FLC	Type 2 Fuzzy Logic Control
T2NFC	Type 2 Neural Fuzzy Control
THD	Total Harmonic Distortion
UL	Underwriters Laboratories Inc
V2D	Vehicle-to-Device
V2G	Vehicle-to-Grid
V2H	Vehicle-to-Home
V2V	Vehicle-to-Vehicle
VDE	Verband Deutscher Elektrotechniker (Germany)

References

1. Element Energy Limited. *Electric Cars: Calculating the Total Cost of Ownership for Consumers*; Element Energy Limited: Cambridge, UK, 2021; p. 44.
2. Habib, S.; Khan, M.M.; Abbas, F.; Sang, L.; Shahid, M.U.; Tang, H. A Comprehensive Study of Implemented International Standards, Technical Challenges, Impacts and Prospects for Electric Vehicles. *IEEE Access* **2018**, *6*, 13866–13890. [[CrossRef](#)]
3. Ahmad, A.; Alam, M.S.; Chabaan, R. A Comprehensive Review of Wireless Charging Technologies for Electric Vehicles. *IEEE Trans. Transp. Electrification* **2017**, *4*, 38–63. [[CrossRef](#)]
4. Trends and Developments in Electric Vehicle Markets—Global EV Outlook 2021—Analysis—IEA. Available online: <https://www.iea.org/reports/global-ev-outlook-2021/trends-and-developments-in-electric-vehicle-markets> (accessed on 25 September 2021).
5. Chakraborty, S.; Vu, H.N.; Hasan, M.M.; Tran, D.D.; El Baghdadi, M.; Hegazy, O. DC-DC converter topologies for electric vehicles, plug-in hybrid electric vehicles and fast charging stations: State of the art and future trends. *Energies* **2019**, *12*, 1569. [[CrossRef](#)]
6. Schmenger, J.; Endres, S.; Zeltner, S.; März, M. A 22 kW on-board charger for automotive applications based on a modular design. In Proceedings of the 2014 IEEE Conference on Energy Conversion (CENCON), Johor Bahru, Malaysia, 13–14 October 2014; pp. 1–6. [[CrossRef](#)]
7. Yang, G.; Lindseth, R.; Sorsdahl, T. Design of High Efficiency High Power Density 10.5 kW Three Phase On-board-charger for Electric/hybrid Vehicles. In Proceedings of the PCIM Europe 2016; International Exhibition and Conference for Power Electronics, Intelligent Motion, Renewable Energy and Energy Management, Nuremberg, Germany, 10–12 May 2016; pp. 10–12.

8. Semsar, S.; Soong, T.; Lehn, P.W. On-Board Single-Phase Integrated Electric Vehicle Charger with V2G Functionality. *IEEE Trans. Power Electron.* **2020**, *35*, 12072–12084. [CrossRef]
9. Tran, V.T.; Rabiul Islam, M.; Muttaqi, K.M.; Sutanto, D. A Novel Universal Magnetic Power Plug to Facilitate V2V/V2G/G2V/V2H Connectivity for Future Grid Infrastructure. In Proceedings of the Conference Record of the IEEE Industry Applications Society Annual Meeting (IAS), Detroit, MI, USA, 10–16 October 2020. [CrossRef]
10. Yilmaz, M.; Krein, P.T. Review of Battery Charger Topologies, Charging Power Levels, and Infrastructure for Plug-In Electric and Hybrid Vehicles. *IEEE Trans. Power Electron.* **2013**, *28*, 2151–2169. [CrossRef]
11. Gao, J.; Jiang, D.; Sun, W.; Zhang, Y. Zero torque three phase integrated on-board charger by multi-elements motor torque cancellation. In Proceedings of the 2019 IEEE Energy Conversion Congress and Exposition (ECCE), Baltimore, MD, USA, 29 September–3 October 2019; pp. 563–568. [CrossRef]
12. Trends in Electric Vehicle Design. Available online: <https://www.mckinsey.com/industries/automotive-and-assembly/our-insights/trends-in-electric-vehicle-design> (accessed on 25 September 2021).
13. Pfund, T.; Gramann, M.; Fritz, M. Efficiency Unlocking with Integrated Power Electronics. *Auto Tech. Rev.* **2014**, *3*, 38–43. [CrossRef]
14. e-Powertrain | NISSAN | Technology. Available online: https://www.nissan-global.com/EN/TECHNOLOGY/OVERVIEW/e_powertrain.html (accessed on 25 September 2021).
15. Powertrain Integration for Electric Vehicles—Power Electronics News. Available online: <https://www.powerelectronicsnews.com/powertrain-integration-for-electric-vehicles/> (accessed on 25 September 2021).
16. Metwally, M.Y.; Abdel-Majeed, M.S.; Abdel-Khalik, A.S.; Hamdy, R.A.; Hamad, M.S.; Ahmed, S. A Review of Integrated On-Board EV Battery Chargers: Advanced Topologies, Recent Developments and Optimal Selection of FSCW Slot/Pole Combination. *IEEE Access* **2020**, *8*, 85216–85242. [CrossRef]
17. Singh, A.K.; Pathak, M.K. A Comprehensive Review of Integrated Charger for on-Board Battery Charging Applications of Electric Vehicles. In Proceedings of the 2018 IEEE 8th Power India International Conference (PIICON), Kurukshetra, India, 10–12 December 2018; Volume 2, pp. 1–6. [CrossRef]
18. Subotic, I.; Levi, E. A review of single-phase on-board integrated battery charging topologies for electric vehicles. In Proceedings of the 2015 IEEE Workshop on Electrical Machines Design, Control and Diagnosis (WEMDCD), Turin, Italy, 26–27 March 2015; pp. 136–145. [CrossRef]
19. Sousa, T.J.C.; Pedrosa, D.; Monteiro, V.; Afonso, J.L. A Review on Integrated Battery Chargers for Electric Vehicles. *Energies* **2022**, *15*, 2756. [CrossRef]
20. Hyundai reveals IONIQ 5 EV for North America—Green Car Congress. Available online: <https://www.greencarcongress.com/2021/05/20210525-ioniq5.html> (accessed on 26 September 2021).
21. B. M. W. M. Information. *Specifications. BMW X3. X3 xDrive30e*; BMW: Munich, Germany, 2019; pp. 1–2.
22. 2021 Nissan Leaf S Hatchback Features and Specs. Available online: https://www.caranddriver.com/nissan/leaf/specs/2021/nissan_leaf_nissan-leaf_2021 (accessed on 26 September 2021).
23. 2021 Volkswagen ID 4 Pro S review: A Good EV Let Down by the Details. Available online: <https://www.cnet.com/roadshow/reviews/2021-volkswagen-id-4-pro-s-rwd-review/> (accessed on 26 September 2021).
24. 2021 Audi e-tron Sportback 50 Quattro Technical Specs, Dimensions. Available online: <https://www.ultimatespecs.com/carspecs/Audi/119216/2021-Audi-e-tron-Sportback-50-quattro.html> (accessed on 26 September 2021).
25. Audi Offering 22-kW Charging On 2021 E-Trons. Available online: <https://www.forbes.com/sites/sebastianblanco/2020/11/28/audi-offering-22-kw-charging-on-2021-e-trons/?sh=5f71b4305c73> (accessed on 26 September 2021).
26. 2020 Renault Zoe R135—Specifications. Available online: <https://www.evspecifications.com/en/model/d323ad> (accessed on 26 September 2021).
27. Mercedes-EQA-2021-Review | LeasePlan. Available online: <https://www.leaseplan.com/en-be/get-inspired/car-review/mercedes-eqa-2021-review/> (accessed on 27 September 2021).
28. Tesla Model Y Long Range Dual Motor Price and Specifications—EV Database. Available online: <https://ev-database.org/car/1182/Tesla-Model-Y-Long-Range-Dual-Motor> (accessed on 27 September 2021).
29. 2021 Tesla Model Y: Photos, Specs & Generations—Forbes Wheels. Available online: <https://www.forbes.com/wheels/cars/tesla/model-y/> (accessed on 27 September 2021).
30. Chevrolet Bolt EV—2021. Available online: <https://media.chevrolet.com/media/us/en/chevrolet/vehicles/bolt-ev/2021.tab1.html> (accessed on 27 September 2021).
31. 2021 Porsche Taycan Turbo S Specifications—The Car Guide. Available online: <https://www.guideautoweb.com/en/makes/porsche/taycan/2021/specifications/turbo-s/> (accessed on 27 September 2021).
32. The Charging Process: Quick, Comfortable, Intelligent and Universal. Available online: <https://newsroom.porsche.com/en/products/taycan/charging-18558.html> (accessed on 27 September 2021).
33. BAIC EC180 EV | Specs | Range | Price | Battery | Pictures | WattEV2Buy. Available online: <https://wattEV2buy.com/electric-vehicles/baic/baic-ec180-ev/> (accessed on 27 September 2021).
34. Chery eQ1 EV | Specs | Range | Battery | Charge Time | Price | WattEV2Buy. Available online: <https://wattEV2buy.com/electric-vehicles/chery-auto/chery-eq1-ev-electric-car/> (accessed on 27 September 2021).
35. JAC iEV7L EV | Specs | Range | Price | Review | Compare | WattEV2Buy. Available online: <https://wattEV2buy.com/electric-vehicles/jac-motors-electric-vehicles/jac-iev7/> (accessed on 27 September 2021).

36. JMC E200S EV | Specs | Range | Battery | Charge Time | Price | WattEV2Buy. Available online: <https://wattEV2buy.com/electric-vehicles/jiangling-motor-corporation-jmc-ev/jmc-e200s-ev-specs-sales-news-pictures-range/> (accessed on 27 September 2021).
37. Khalid, M.R.; Khan, I.A.; Hameed, S.; Asghar, M.S.J.; Ro, J.S. A Comprehensive Review on Structural Topologies, Power Levels, Energy Storage Systems, and Standards for Electric Vehicle Charging Stations and Their Impacts on Grid. *IEEE Access* **2021**, *9*, 128069–128094. [[CrossRef](#)]
38. Nguyen, H.V.; Lee, D.C.; Blaabjerg, F. A Novel SiC-Based Multifunctional Onboard Battery Charger for Plug-In Electric Vehicles. *IEEE Trans. Power Electron.* **2021**, *36*, 5635–5646. [[CrossRef](#)]
39. Nguyen, H.V.; To, D.D.; Lee, D.C. Onboard Battery Chargers for Plug-in Electric Vehicles with Dual Functional Circuit for Low-Voltage Battery Charging and Active Power Decoupling. *IEEE Access* **2018**, *6*, 70212–70222. [[CrossRef](#)]
40. Su, G.J.; Tang, L. An integrated onboard charger and accessory power converter using WBG devices. In Proceedings of the 2015 IEEE Energy Conversion Congress and Exposition (ECCE), Montreal, QC, Canada, 20–24 September 2015; pp. 6306–6313. [[CrossRef](#)]
41. Kim, Y.S.; Oh, C.Y.; Sung, W.Y.; Lee, B.K. Topology and Control Scheme of OBC-LDC Integrated Power Unit for Electric Vehicles. *IEEE Trans. Power Electron.* **2017**, *32*, 1731–1743. [[CrossRef](#)]
42. Kwon, M.; Choi, S. An Electrolytic Capacitorless Bidirectional EV Charger for V2G and V2H Applications. *IEEE Trans. Power Electron.* **2017**, *32*, 6792–6799. [[CrossRef](#)]
43. Pinto, J.G.; Monteiro, V.; Gonçalves, H.; Afonso, J.L. Onboard reconfigurable battery charger for electric vehicles with traction-to-auxiliary mode. *IEEE Trans. Veh. Technol.* **2014**, *63*, 1104–1116. [[CrossRef](#)]
44. Nam, V.-H.; Tinh, D.-V.; Choi, W. A Novel Hybrid LDC Converter Topology for the Integrated On-Board Charger of Electric Vehicles. *Energies* **2021**, *14*, 3603. [[CrossRef](#)]
45. Winning the Chinese Electric Car Market | McKinsey. Available online: <https://www.mckinsey.com/industries/automotive-and-assembly/our-insights/winning-the-chinese-bev-market-how-leading-international-oems-compete> (accessed on 18 February 2022).
46. Chiang, G.T.; Shuji, T.; Takahide, S.; Kitamura, Y.; Fukada, M.; Handa, Y. Proposal of integrated circuit structure with boost motor drive and on-board charging for a 48V battery system. In Proceedings of the 2019 21st European Conference on Power Electronics and Applications (EPE'19 ECCE Europe), Genova, Italy, 3–5 September 2019; pp. 1–10. [[CrossRef](#)]
47. Singh, S.A.; Carli, G.; Azeez, N.A.; Williamson, S.S. Modeling, Design, Control, and Implementation of a Modified Z-Source Integrated PV/Grid/EV DC Charger/Inverter. *IEEE Trans. Ind. Electron.* **2018**, *65*, 5213–5220. [[CrossRef](#)]
48. Li, W.; Yuan, Z.; Lai, B.; Zhang, Q. A control method of three-phase Z-source integrated charger with motor windings. In Proceedings of the 2018 13th IEEE Conference on Industrial Electronics and Applications (ICIEA), Wuhan, China, 31 May–2 June 2018; pp. 1721–1726. [[CrossRef](#)]
49. Na, T.; Yuan, X.; Tang, J.; Zhang, Q. A review of on-board integrated charger for electric vehicles and a new solution. In Proceedings of the 2019 IEEE 10th International Symposium on Power Electronics for Distributed Generation Systems (PEDG), Xi'an, China, 3–6 June 2019; Volume 4, pp. 693–699. [[CrossRef](#)]
50. Pan, L.; Zhang, C. An integrated multifunctional bidirectional AC/DC and DC/DC converter for electric vehicles applications. *Energies* **2016**, *9*, 493. [[CrossRef](#)]
51. Su, G.J.; Tang, L. Current source inverter based traction drive for EV battery charging applications. In Proceedings of the 011 IEEE vehicle power and propulsion conference, Chicago, IL, USA, 6–9 September 2011; pp. 1–6. [[CrossRef](#)]
52. Rodrigues, M.C.B.P.; Souza, I.D.N.; Ferreira, A.A.; Barbosa, P.G.; Braga, H.A.C. Simultaneous active power filter and G2V (or V2G) operation of EV on-board power electronics. In Proceedings of the IECO 2013-39th Annual Conference of the IEEE Industrial Electronics Society, Vienna, Austria, 10–13 November 2013; pp. 4684–4689. [[CrossRef](#)]
53. Foti, S.; Testa, A.; Scimone, T.; De Caro, S.; Scelba, G.; Tornello, L.D. An integrated battery charger for EV applications based on an open end winding multilevel converter configuration. In Proceedings of the 2019 21st European Conference on Power Electronics and Applications (EPE'19 ECCE Europe), Genova, Italy, 3–5 September 2019; pp. 1–8. [[CrossRef](#)]
54. Vitesco Technologies—High Voltage Box. Available online: <https://www.vitesco-technologies.com/en-us/products/high-voltage-box> (accessed on 18 February 2022).
55. 11KW OBC+3KW DC/DC Converter Bidirectional—Industrial Battery Charger Manufacturer. Available online: <https://www.aodicharger.com/11kw-obc-bidirectional-charging.html> (accessed on 18 February 2022).
56. Charger-Inverter, a Specific Solution for Electric Vehicles | Valeo. Available online: <https://www.valeo.com/en/charger-inverter/> (accessed on 18 February 2022).
57. Graf, F.; Brüll, M.; Deinhard, S. AllCharge™—A user-centric solution for traction and charging. In Proceedings of the Der Antrieb von Morgen 2018; Springer Vieweg: Wiesbaden, Germany, 2018; pp. 33–49. [[CrossRef](#)]
58. Hegazy, O.; van Mierlo, J.; Lataire, P. Control and analysis of an integrated bidirectional DC/AC AND DC/DC converters for plug-in hybrid electric vehicle applications. *J. Power Electron.* **2011**, *11*, 408–417. [[CrossRef](#)]
59. Song, H.S.; Yoo, I.P.; Jang, K.Y.; Shin, S.; Joo, J.H. System for Recharging Plug-in Electric Vehicle and Control Method for the Same. U.S. Patent US 8441229 B2, 2 May 2013.
60. Sarrazin, B. *Optimisation d'une Chaîne de Traction pour Véhicule Électrique*. *Energie Électrique*; (NNT: 2012GRENT117). (tel-00808946v2); Université de Grenoble: Saint-Martin-d'Hères, France, 2012. (In Français)
61. Gupta, J.; Maurya, R.; Arya, S.R. Improved Power Quality On-Board Integrated Charger with Reduced Switching Stress. *IEEE Trans. Power Electron.* **2020**, *35*, 10810–10820. [[CrossRef](#)]

62. Woo, D.G.; Joo, D.M.; Lee, B.K. On the Feasibility of Integrated Battery Charger Utilizing Traction Motor and Inverter in Plug-In Hybrid Electric Vehicles. *IEEE Trans. Power Electron.* **2015**, *30*, 7270–7281. [[CrossRef](#)]
63. Tang, L.; Su, G.J. Control scheme optimization for a low-cost, digitally-controlled charger for plug-in hybrid electric vehicles. In Proceedings of the 2009 IEEE Energy Conversion Congress and Exposition, San Jose, CA, USA, 20–24 September 2009; pp. 3604–3610. [[CrossRef](#)]
64. Subotic, I.; Jones, M.; Levi, E. A fast on-board integrated battery charger for four-motor EVs. In Proceedings of the 2014 International Conference on Electrical Machines (ICEM), Berlin, Germany, 2–5 September 2014; pp. 2066–2072. [[CrossRef](#)]
65. Sul, S.K.; Lee, S.J. An Integral Battery Charger for Four-Wheel Drive Electric Vehicle. *IEEE Trans. Ind. Appl.* **1995**, *31*, 1096–1099. [[CrossRef](#)]
66. Khan, M.A.; Husain, I.; Sozer, Y. Integrated electric motor drive and power electronics for bidirectional power flow between electric vehicle and DC or AC grid. In Proceedings of the IEEE Energy Conversion Congress and Exposition, ECCE, Raleigh, NC, USA, 15–20 September 2012; pp. 3403–3410. [[CrossRef](#)]
67. Tuan, V.T.; Phattanasak, M.; Kreuawan, S. Integrated charger-inverter for high-performance electric motorcycles. *World Electr. Veh. J.* **2021**, *12*, 19. [[CrossRef](#)]
68. Khayam Huseini, S.R.; Farjah, E.; Tashakor, N.; Ghanbari, T. Development of an integrated Switched-Reluctance Motor drive with battery charging capability for electric vehicle propulsion system. In Proceedings of the 6th Power Electronics, Drive Systems & Technologies Conference (PEDSTC2015), Tehran, Iran, 3–4 February 2015; pp. 579–584. [[CrossRef](#)]
69. Hu, K.W.; Yi, P.H.; Liaw, C.M. An EV SRM Drive Powered by Battery/Supercapacitor with G2V and V2H/V2G Capabilities. *IEEE Trans. Ind. Electron.* **2015**, *62*, 4714–4727. [[CrossRef](#)]
70. Shi, C.; Tang, Y.; Khaligh, A. A Three-Phase Integrated Onboard Charger for Plug-In Electric Vehicles. *IEEE Trans. Power Electron.* **2018**, *33*, 4716–4725. [[CrossRef](#)]
71. De Sousa, L.; Silvestre, B.; Bouchez, B. A combined multiphase electric drive and fast battery charger for electric vehicles: Topology and electric propulsion efficiency analysis. In Proceedings of the 2010 IEEE Vehicle Power and Propulsion Conference, Lille, France, 1–3 September 2010. [[CrossRef](#)]
72. Sandulescu, A.P.; Meinguet, F.; Kestelyn, X.; Semail, E.; Bruyere, A. Flux-weakening operation of open-end winding drive integrating a cost-effective high-power charger. *IET Electr. Syst. Transp.* **2013**, *3*, 10–21. [[CrossRef](#)]
73. Lacroix, S.; Laboure, E.; Hilairret, M. An integrated fast battery charger for electric vehicle. In Proceedings of the 2010 IEEE Vehicle Power and Propulsion Conference, Lille, France, 1–3 September 2010; pp. 1–6. [[CrossRef](#)]
74. Haghbin, S.; Carlson, O. Integrated motor drive and non-isolated battery charger based on the split-phase PM motors for plug-in vehicles. *J. Eng.* **2014**, *2014*, 275–283. [[CrossRef](#)]
75. Bruyère, A.; De Sousa, L.; Bouchez, B.; Sandulescu, P.; Kestelyn, X.; Semail, E. A multiphase traction/fast-battery-charger drive for electric or plug-in hybrid vehicles: Solutions for control in traction mode. In Proceedings of the 2010 IEEE Vehicle Power and Propulsion Conference, Lille, France, 1–3 September 2010; pp. 1–7. [[CrossRef](#)]
76. Bruell, M.; Brockerhoff, P.; Pfeilschifter, F.; Feustel, H.P.; Hackmann, W. Bidirectional charge- and traction-system. *World Electr. Veh. J.* **2016**, *8*, 237–248. [[CrossRef](#)]
77. Sharma, S.; Aware, M.V.; Bhowate, A. Integrated Battery Charger for EV by Using Three-Phase Induction Motor Stator Windings as Filter. *IEEE Trans. Transp. Electr.* **2020**, *6*, 83–94. [[CrossRef](#)]
78. Chon, C.; Duck, K.; Jung, H.; Tae, H.; Noh, S.H. Multi-Input Charging System and Method Using Motor Driving System 2020. Available online: <https://www.freepatentsonline.com/y2020/0361323.html> (accessed on 1 October 2021).
79. Scelba, G.; Scarcella, G.; Foti, S.; De Caro, S.; Testa, A. Self-sensing control of open-end winding PMSMS fed by an asymmetrical hybrid multilevel inverter. In Proceedings of the 2017 IEEE International Symposium on Sensorless Control for Electrical Drives (SLED), Catania, Italy, 18–19 September 2017; pp. 165–172. [[CrossRef](#)]
80. Hoevenaars, E.; Illg, T.; Hiller, M. Novel integrated charger concept using an induction machine as transformer at standstill. In Proceedings of the 2020 IEEE Vehicle Power and Propulsion Conference (VPPC), Gijon, Spain, 18 November–16 December 2020. [[CrossRef](#)]
81. Asymmetrical, T.I.; Pmsm, S. Common-Mode Voltage Elimination for Dual. *IEEE Trans. Power Electron.* **2020**, *35*, 3828–3840.
82. Han, X.; Jiang, D.; Zou, T.; Qu, R.; Yang, K. Two-Segment Three-Phase PMSM Drive with Carrier Phase-Shift PWM for Torque Ripple and Vibration Reduction. *IEEE Trans. Power Electron.* **2018**, *34*, 588–599. [[CrossRef](#)]
83. Raherimihaja, H.J.; Zhang, F.; Na, T.; Zhang, Q. An integrated charger using segmented windings of interior permanent magnet motor based on 3 phase with 9 windings. In Proceedings of the 2018 13th IEEE Conference on Industrial Electronics and Applications (ICIEA), Wuhan, China, 31 May–2 June 2018; pp. 565–570. [[CrossRef](#)]
84. Szenasy, I.; Varga, Z. Features of segment winded PMSM for a low voltage supply system. In Proceedings of the 2017 3rd International Conference on Control, Automation and Robotics (ICCAR), Nagoya, Japan, 24–26 April 2017; pp. 523–528. [[CrossRef](#)]
85. Abdel-Khalik, A.S.; Ahmed, S.; Massoud, A.M. A Nine-Phase Six-Terminal Concentrated Single-Layer Winding Layout for High-Power Medium-Voltage Induction Machines. *IEEE Trans. Ind. Electron.* **2017**, *64*, 1796–1806. [[CrossRef](#)]
86. Bodo, N.; Levi, E.; Subotic, I.; Espina, J.; Empringham, L.; Johnson, C.M. Efficiency Evaluation of Fully Integrated On-Board EV Battery Chargers With Nine-Phase Machines. *IEEE Trans. Energy Convers.* **2017**, *32*, 257–266. [[CrossRef](#)]
87. Diab, M.S.; Elserougi, A.A.; Abdel-Khalik, A.S.; Massoud, A.M.; Ahmed, S. A Nine-Switch-Converter-Based Integrated Motor Drive and Battery Charger System for EVs Using Symmetrical Six-Phase Machines. *IEEE Trans. Ind. Electron.* **2016**, *63*, 5326–5335. [[CrossRef](#)]
88. Subotic, I.; Bodo, N.; Levi, E. An EV Drive-Train With Integrated Fast Charging Capability. *IEEE Trans. Power Electron.* **2016**, *31*, 1461–1471. [[CrossRef](#)]

89. Subotic, I.; Levi, E.; Jones, M.; Graovac, D. Multiphase integrated on-board battery chargers for electrical vehicles. In Proceedings of the 2013 15th European Conference on Power Electronics and Applications (EPE), Lille, France, 2–6 September 2013; pp. 1–10. [\[CrossRef\]](#)
90. Tong, M.; Cheng, M.; Wang, S.; Hua, W. An On-Board Two-Stage Integrated Fast Battery Charger for EVs Based on a Five-Phase Hybrid-Excitation Flux-Switching Machine. *IEEE Trans. Ind. Electron.* **2021**, *68*, 1780–1790. [\[CrossRef\]](#)
91. Subotic, I.; Bodo, N.; Levi, E.; Jones, M.; Levi, V. Isolated chargers for EVs incorporating six-phase machines. *IEEE Trans. Ind. Electron.* **2016**, *63*, 653–664. [\[CrossRef\]](#)
92. Haghbin, S.; Lundmark, S.; Alaküla, M.; Carlson, O. An isolated high-power integrated charger in electrified-vehicle applications. *IEEE Trans. Veh. Technol.* **2011**, *60*, 4115–4126. [\[CrossRef\]](#)
93. Abdel-Khalik, A.S.; Massoud, A.; Ahmed, S. Interior permanent magnet motor-based isolated on-board integrated battery charger for electric vehicles. *IET Electr. Power Appl.* **2018**, *12*, 124–134. [\[CrossRef\]](#)
94. Pescetto, P.; Pellegrino, G. Integrated Isolated OBC for EVs with 6-phase Traction Motor Drives. In Proceedings of the 2020 IEEE Energy Conversion Congress and Exposition (ECCE), Detroit, MI, USA, 11–15 October 2020; pp. 4112–4117. [\[CrossRef\]](#)
95. De Klerk, M.L.; Saha, A.K. A Comprehensive Review of Advanced Traction Motor Control Techniques Suitable for Electric Vehicle Applications. *IEEE Access* **2021**, *9*, 125080–125108. [\[CrossRef\]](#)
96. Cai, W.; Wu, X.; Zhou, M.; Liang, Y.; Wang, Y. Review and Development of Electric Motor Systems and Electric Powertrains for New Energy Vehicles. *Automot. Innov.* **2021**, *4*, 3–22. [\[CrossRef\]](#)
97. Huang, S.J.; Huang, B.G.; Pai, F.S. Fast charge strategy based on the characterization and evaluation of LiFePO₄ batteries. *IEEE Trans. Power Electron.* **2013**, *28*, 1555–1562. [\[CrossRef\]](#)
98. Chen, L.R. Design of duty-varied voltage pulse charger for improving Li-ion battery-charging response. *IEEE Trans. Ind. Electron.* **2009**, *56*, 480–487. [\[CrossRef\]](#)
99. Adiga, P.S.; Kumar, H.; Iyer, S.R.; Arjun, M.; Dsouza, R.C.; Venkatesaperumal, B. A PFC Hysteresis Current Controller for Totem-pole Bridgeless Bi-directional EV charger. In Proceedings of the 2022 IEEE International Conference on Power Electronics, Smart Grid, and Renewable Energy (PESGRE), Trivandrum, India, 2–5 January 2022; pp. 31–34. [\[CrossRef\]](#)
100. Bak, Y.; Kang, H.S. Control methods for performance improvement of an integrated on-board battery charger in hybrid electric vehicles. *Electronics* **2021**, *10*, 2506. [\[CrossRef\]](#)
101. Pan, L.; Zhang, C. Performance Enhancement of Battery Charger for Electric Vehicles Using Resonant Controllers. *Energy Procedia* **2017**, *105*, 3990–3996. [\[CrossRef\]](#)
102. Hegazy, O.; El Baghdadi, M.; Van Mierlo, J.; Lataire, P. Modeling and analysis of different control techniques of conductive battery chargers for electric vehicles applications. *Int. J. Comput. Math. Electr. Electron. Eng.* **2015**, *34*, 151–172. [\[CrossRef\]](#)
103. Kouros, S.; Cortés, P.; Vargas, R.; Ammann, U.; Rodríguez, J. Model predictive control—A simple and powerful Method to control power converters. *IEEE Trans. Ind. Electron.* **2009**, *56*, 1826–1838. [\[CrossRef\]](#)
104. Jun, E.S.; Kwak, S.; Kim, T. Performance comparison of model predictive control methods for active front end rectifiers. *IEEE Access* **2018**, *6*, 77272–77288. [\[CrossRef\]](#)
105. Rodríguez, J.; Kazmierkowski, M.P.; Espinoza, J.R.; Zanchetta, P.; Abu-Rub, H.; Young, H.A.; Rojas, C.A. State of the art of finite control set model predictive control in power electronics. *IEEE Trans. Ind. Inform.* **2013**, *9*, 1003–1016. [\[CrossRef\]](#)
106. Zhao, R.; Chang, Z.; Yuan, P.; Yang, L.; Li, Z. A novel fuzzy logic and anti-windup PI controller for three-phase grid connected inverter. In Proceedings of the 2009 2nd International Conference on Power Electronics and Intelligent Transportation System (PEITS), Melaka, Malaysia, 28–29 November 2016; Volume 1, pp. 442–446. [\[CrossRef\]](#)
107. Ahmed, K.Y.; Yahaya, N.Z.; Asirvadam, V.S.; Ramani, K.; Ibrahim, O. Comparison of fuzzy logic control and PI control for a three-level rectifier based on voltage oriented control. In Proceedings of the 2016 IEEE International Conference on Power and Energy (PECon), Shenzhen, China, 19–20 December 2009; pp. 127–132. [\[CrossRef\]](#)
108. Zeb, K.; Islam, S.U.; Din, W.U.; Khan, I.; Ishfaq, M.; Busarello, T.D.C.; Ahmad, I.; Kim, H.J. Design of fuzzy-PI and fuzzy-sliding mode controllers for single-phase two-stages grid-connected transformerless photovoltaic inverter. *Electronics* **2019**, *8*, 520. [\[CrossRef\]](#)
109. Azli, N.A.; Wong, S.N. Development of a DSP-based fuzzy PI controller for an online optimal PWM control scheme for a multilevel inverter. In Proceedings of the 2005 International Conference on Power Electronics and Drives Systems, Kuala Lumpur, Malaysia, 28 November–1 December 2005; Volume 2, pp. 1457–1461. [\[CrossRef\]](#)
110. Kumar, M.; Singh, B.; Singh, B.P. Fuzzy Pre-compensated PI Controller for PMBLDC Motor Drive. In Proceedings of the 2006 International Conference on Power Electronic, Drives and Energy Systems, Delhi, India, 12–15 December 2006; pp. 1–5. [\[CrossRef\]](#)
111. Zheng, Z.; Tao, H.J. Research of three-phase PWM rectifier based on PI control with auto-tuning scaling factors. In Proceedings of the 2006 6th World Congress on Intelligent Control and Automation, Dalian, China, 21–23 June 2006; Volume 1, pp. 3844–3847. [\[CrossRef\]](#)
112. Liu, G.; Li, L. Quantification factor self-tuning fuzzy PID controller research for a permanent magnet synchronous motor feeding system. In Proceedings of the 2012 24th Chinese Control and Decision Conference (CCDC), Taiyuan, China, 23–25 May 2012; pp. 2510–2514. [\[CrossRef\]](#)
113. Liu, W.; Liu, L.; Cartes, D.A.; Wang, X. Neural network based controller design for three-phase PWM AC/DC voltage source converters. In Proceedings of the 2008 IEEE International Joint Conference on Neural Networks (IEEE World Congress on Computational Intelligence), Hong Kong, China, 1–8 June 2008; pp. 3421–3427. [\[CrossRef\]](#)
114. Li, S.; Fairbank, M.; Johnson, C.; Wunsch, D.C.; Alonso, E.; Proao, J.L. Artificial neural networks for control of a grid-connected rectifier/inverter under disturbance, dynamic and power converter switching conditions. *IEEE Trans. Neural Netw. Learn. Syst.* **2014**, *25*, 738–750. [\[CrossRef\]](#)

115. Cecati, C.; Dell'Aquila, A.; Lecci, A.; Liserre, M. Implementation issues of a fuzzy-logic-based three-phase active rectifier employing only voltage sensors. *IEEE Trans. Ind. Electron.* **2005**, *52*, 378–385. [[CrossRef](#)]
116. Cetin, O.; Kurnaz, S.; Kaynak, O. Fuzzy logic based approach to design of autonomous landing system for unmanned aerial vehicles. *J. Intell. Robot. Syst. Theory Appl.* **2011**, *61*, 239–250. [[CrossRef](#)]
117. Gunes, M.; Dogru, N. Fuzzy control of brushless excitation system for steam turbogenerators. *IEEE Trans. Energy Convers.* **2010**, *25*, 844–852. [[CrossRef](#)]
118. Acikgoz, H.; Kumar, A.; Beiranvand, H.; Sekkeli, M. Hardware implementation of type-2 neuro-fuzzy controller-based direct power control for three-phase active front-end rectifiers. *Int. Trans. Electr. Energy Syst.* **2019**, *29*, e12066. [[CrossRef](#)]
119. Abiyev, R.H.; Kaynak, O. Type 2 fuzzy neural structure for identification and control of time-varying plants. *IEEE Trans. Ind. Electron.* **2010**, *57*, 4147–4159. [[CrossRef](#)]
120. Coteli, R.; Acikgoz, H.; Ucar, F.; Dandil, B. Design and implementation of Type-2 fuzzy neural system controller for PWM rectifiers. *Int. J. Hydrog. Energy* **2017**, *42*, 20759–20771. [[CrossRef](#)]
121. Emadi, A.; Williamson, S.S.; Khaligh, A. Power electronics intensive solutions for advanced electric, hybrid electric, and fuel cell vehicular power systems. *IEEE Trans. Power Electron.* **2006**, *21*, 567–577. [[CrossRef](#)]
122. Maggetto, G.; Van Mierlo, J. Electric and electric hybrid vehicle technology: A survey. In Proceedings of the IEE Seminar on Electric, Hybrid and Fuel Cell Vehicle, Durham, UK, 11 April 2000; pp. 1–11. [[CrossRef](#)]
123. Zeraoulia, M.; Benbouzid, M.E.H.; Diallo, D. Electric motor drive selection issues for HEV propulsion systems: A comparative study. *IEEE Trans. Veh. Technol.* **2006**, *55*, 1756–1764. [[CrossRef](#)]
124. Chan, C.C.; Bouscayrol, A.; Chen, K. Electric, hybrid, and fuel-cell vehicles: Architectures and modeling. *IEEE Trans. Veh. Technol.* **2010**, *59*, 589–598. [[CrossRef](#)]
125. Hegazy, O.; Lataire, P. Modeling and Analysis of Different Control Techniques of Electric Motor for Electric Vehicle Powertrains. *EPE J.* **2015**, *25*, 36–46. [[CrossRef](#)]
126. Amin, A.M.A.; El Korfally, M.I.; Sayed, A.A.; Hegazy, O.T.M. Efficiency optimization of two-asymmetrical-winding induction motor based on swarm intelligence. *IEEE Trans. Energy Convers.* **2009**, *24*, 12–20. [[CrossRef](#)]
127. Hegazy, O.; Barrero, R.; Van Mierlo, J.; Lataire, P.; Omar, N.; Coosemans, T. An Advanced Power Electronics Interface for Electric Vehicles Applications. *IEEE Trans. Power Electron.* **2013**, *28*, 5508–5521. [[CrossRef](#)]
128. Sergaki, E.S.; Essounbouli, N.; Kalaitzakis, K.C.; Stavrakakis, G.S. Fuzzy logic control for motor flux reduction during steady states and for flux recovery in transient states of indirect-FOC AC drives. In Proceedings of the The XIX International Conference on Electrical Machines-ICEM 2010, Rome, Italy, 6–8 September 2010. [[CrossRef](#)]
129. Zeb, K.; Ali, Z.; Saleem, K.; Uddin, W.; Javed, M.A.; Christofides, N. Indirect field-oriented control of induction motor drive based on adaptive fuzzy logic controller. *Electr. Eng.* **2017**, *99*, 803–815. [[CrossRef](#)]
130. El Badsy, B.; Bouzidi, B.; Masmoudi, A. Bus-clamping-based DTC: An attempt to reduce harmonic distortion and switching losses. *IEEE Trans. Ind. Electron.* **2013**, *60*, 873–884. [[CrossRef](#)]
131. Karamanakos, P.; Stolze, P.; Kennel, R.M.; Manias, S.; Du Toit Mouton, H. Variable Switching Point Predictive Torque Control of Induction Machines. *IEEE J. Emerg. Sel. Top. Power Electron.* **2014**, *2*, 285–295. [[CrossRef](#)]
132. Buja, G.S.; Kazmierkowski, M.P. Direct torque control of PWM inverter-fed AC motors—A survey. *IEEE Trans. Ind. Electron.* **2004**, *51*, 744–757. [[CrossRef](#)]
133. Belhaouchet, N.; Hamla, H.; Rahmani, L. A modified direct torque control for induction motor drives. *Rev. Roum. Sci. Tech. Ser. Electrotech. Energy* **2018**, *63*, 38–45.
134. Li, H. Fuzzy DTC for induction motor with optimized command stator flux. In Proceedings of the 2010 8th World Congress on Intelligent Control and Automation, Jinan, China, 7–9 July 2010; pp. 4958–4961. [[CrossRef](#)]
135. Muddineni, V.P.; Sandepudi, S.R.; Bonala, A.K. Predictive torque control of induction motor drive with simplified weighting factor selection. In Proceedings of the 2016 IEEE International Conference on Power Electronics, Drives and Energy Systems (PEDES), Trivandrum, India, 14–17 December 2016; pp. 1–6. [[CrossRef](#)]
136. Wang, F.; Mei, X.; Rodriguez, J.; Kennel, R. Model predictive control for electrical drive systems—an overview. *CES Trans. Electr. Mach. Syst.* **2020**, *1*, 219–230. [[CrossRef](#)]
137. Wróbel, K.; Serkies, P.; Szabat, K. Continuous and Finite Set Model Predictive Control of Induction Motor Drive. In Proceedings of the IECON 2019-45th Annual Conference of the IEEE Industrial Electronics Society, Lisbon, Portugal, 14–17 October 2019; pp. 963–968. [[CrossRef](#)]
138. Zhang, Y.; Xia, B.; Yang, H.; Rodriguez, J. Overview of model predictive control for induction motor drives. *Chin. J. Electr. Eng.* **2016**, *2*, 62–76. [[CrossRef](#)]
139. Uddin, M.; Mekhilef, S.; Nakaoka, M.; Rivera, M. Model predictive control of induction motor with delay time compensation: An experimental assessment. In Proceedings of the 2015 IEEE Applied Power Electronics Conference and Exposition (APEC), Charlotte, NC, USA, 15–19 March 2015; pp. 543–548. [[CrossRef](#)]
140. Jadhav, M.S.V.; Kirankumar, M.J.; Chaudhari, D.B.N. ANN based Intelligent Control of Induction Motor drive with Space Vector Modulated DTC. In Proceedings of the International Conference on Power Electronics, Drives and Energy Systems, Bengaluru, India, 16–19 December 2012. [[CrossRef](#)]

141. Falvo, M.C.; Sbordone, D.; Bayram, I.S.; Devetsikiotis, M. EV charging stations and modes: International standards. In Proceedings of the 2014 International Symposium on Power Electronics, Electrical Drives, Automation and Motion, Ischia, Italy, 18–20 June 2014; pp. 1134–1139. [[CrossRef](#)]
142. Foley, A.M. State-of-the-Art in Electric Vehicle Charging Infrastructure. In Proceedings of the 2010 IEEE Vehicle Power and Propulsion Conference, Lille, France, 1–3 September 2010.
143. Lu, M.H.; Jen, M.U. Safety design of electric vehicle charging equipment. *World Electr. Veh. J.* **2012**, *5*, 1017–1024. [[CrossRef](#)]
144. IEC 60990:2016 RLV; Methods of Measurement of Touch Current and Protective Conductor Current. Edition 3. International Electrotechnical Commission (IEC): Geneva, Switzerland, 2016. Available online: <https://webstore.iec.ch/publication/24974> (accessed on 25 March 2022).
145. Zhang, Y.; Chen, C.; Perdikakis, W.; Cong, Y.; Li, X.; Elshaer, M.; Abdullah, Y.; Wang, J.; Zou, K.; Xu, Z. Leakage current mitigation of non-isolated integrated chargers for electric vehicles. In Proceedings of the 2019 IEEE Energy Conversion Congress and Exposition (ECCE), Baltimore, MD, USA, 29 September–3 October 2019; pp. 1195–1201. [[CrossRef](#)]
146. ISO 20200:2004; International Standard. 61010-1 © Iec2001. ISO: Geneva, Switzerland, 2003.
147. Sharma, A.; Sharma, S. Review of power electronics in vehicle-to-grid systems. *J. Energy Storage* **2019**, *21*, 337–361. [[CrossRef](#)]
148. Anwar, M.; Alam, M.K.; Gleason, S.E.; Setting, J. Traction power inverter design for EV and HEV applications at general motors: A review. In Proceedings of the 2019 IEEE Energy Conversion Congress and Exposition (ECCE), Baltimore, MD, USA, 29 September–3 October 2019; pp. 6346–6351. [[CrossRef](#)]
149. Reimers, J.; Dorn-Gomba, L.; Mak, C.; Emadi, A. Automotive Traction Inverters: Current Status and Future Trends. *IEEE Trans. Veh. Technol.* **2019**, *68*, 3337–3350. [[CrossRef](#)]
150. Husain, I.; Ozpineci, B.; Islam, M.S.; Gurpinar, E.; Su, G.J.; Yu, W.; Chowdhury, S.; Xue, L.; Rahman, D.; Sahu, R. Electric Drive Technology Trends, Challenges, and Opportunities for Future Electric Vehicles. *Proc. IEEE* **2021**, *109*, 1039–1059. [[CrossRef](#)]
151. Chowdhury, S.; Gurpinar, E.; Su, G.J.; Raminosoa, T.; Burrell, T.A.; Ozpineci, B. Enabling Technologies for Compact Integrated Electric Drives for Automotive Traction Applications. In Proceedings of the 2019 IEEE Transportation Electrification Conference and Expo (ITEC), Detroit, MI, USA, 19–21 June 2019. [[CrossRef](#)]
152. Popescu, M.; Goss, J.; Staton, D.A.; Hawkins, D.; Chong, Y.C.; Boglietti, A. Electrical Vehicles—Practical Solutions for Power Traction Motor Systems. *IEEE Trans. Ind. Appl.* **2018**, *54*, 2751–2762. [[CrossRef](#)]
153. Feurtado, M.; McPherson, B.; Martin, D.; McNutt, T.; Schupbach, M.; Curbow, W.A.; Hayes, J.; Sparkman, B. 143_300kWINV.pdf. PCIM Europe 2019; International Exhibition and Conference for Power Electronics, Intelligent Motion, Renewable Energy and Energy Management. Available online: <https://ieeexplore.ieee.org/abstract/document/8767734/authors#authors> (accessed on 30 March 2022).